2008

CHARACTERIZATION OF TWO METAVINCULIN MUTATIONS

W. Luke Henderson
Western University

CHARACTERIZATION OF TWO METAVINCULIN MUTATIONS

(Thesis format: Monograph)

by

W. Luke Henderson

Graduate Program in the
Department of Biochemistry

A thesis submitted in partial fulfillment
of the requirements for the degree of
Master of Science

Faculty of Graduate Studies
The University of Western Ontario
London, Ontario, Canada

ABSTRACT

Vinculin is a cytoskeletal protein which localizes to adherens junctions that occur between adjoining cells. A muscle-specific splice variant metavinculin is identical in sequence to vinculin with the exception of a 68-residue insert within its C-terminal domain. Two mutations (R975W and L954del) within this insert have been associated with the onset of dilated cardiomyopathy. This study investigated structural differences among the wild-type and mutant metavinculin tail domains, and also examined differences in binding characteristics among known ligands. Structural studies indicated that the mutations do not induce large conformational changes on the metavinculin tail, though they may result in reduced exposed hydrophobic surface, and the R975W mutant was found to show slightly decreased thermal stability. Interactions of wild-type and mutant proteins with the vinculin head, acidic phospholipids, EVH1, and actin were shown to be similar. In addition, viscometric analysis indicated a synergistic effect of vinculin-metavinculin heterodimerization on filamentous actin network formation.

Keywords: metavinculin, mutations, dilated cardiomyopathy, actin, phospholipid, conformational change, vinculin, dimerization

TABLE OF CONTENTS

CERTIFICATE OF EXAMINATION.....ii

ABSTRACT.....iii

DEDICATION.....iv

ACKNOWLEDGEMENTS.....v

TABLE OF CONTENTS.....vi

LIST OF FIGURES.....ix

LIST OF TABLES.....xi

LIST OF ABBREVIATIONS.....xii

CHAPTER 1 – INTRODUCTION.....1

1.1 Overview.....1

1.2 Vinculin.....1

1.2.1 Structure and Regulation.....1

1.2.2 Function.....4

1.3 Metavinculin.....7

1.3.1 Sequence and Role.....7

1.3.2 Cardiomyopathic Mutations.....11

1.4 Purpose of Thesis.....13

CHAPTER 2 – EXPERIMENTAL PROCEDURES.....14

2.1 Cloning and Mutagenesis.....14

2.1.1 N-terminal GST-fusion constructs.....14

2.1.2 N-terminal cysteine constructs.....14

2.1.3 Mvt 833 constructs.....15

2.2 Protein Expression and Purification.....16

2.2.1 Thioredoxin Fusions.....17

2.2.1.1 Metavinculin/Vinculin Tail.....18

2.2.1.2 Vinculin Head.....19

2.2.2 GST-Fusions.....20

2.2.2.1 Metavinculin Tail.....20

2.2.2.2 EVH1 Domain.....20

2.2.3 Labelling with Fluorescent Molecules.....21

2.3 Circular Dichroism Melting Curves.....21

2.4 Protease K Proteolysis.....22

2.5 ANS Emission Spectra.....22

2.6 Phenylsepharose Binding Assay.....22

2.7 Fluorescent Head-Tail Competitive Binding Assay.....23

2.8 Lipid Cosedimentation Assays.....24

2.9 PIP Strip Overlay Assays.....24

2.10 Actin Cosedimentation Assays.....25

2.11 Falling Ball Viscometry.....25

2.12 Nitrocellulose Overlay Assays.....26

2.13 Gel Filtration.....27

2.14 Western Blotting of Tissue Extracts.....27

2.15 Binding of Metavinculin to Permeabilized Cells.....28

2.16 Other Techniques.....28

CHAPTER 3 – RESULTS.....30

3.1 Physical Properties of Wild-Type and Mutant Metavinculin.....30

3.2 Biological Properties and Interactions of Metavinculin.....36

CHAPTER 4 – DISCUSSION.....54

4.1 Physical Properties of Wild-Type and Mutant Metavinculin.....54

4.2 Biological Properties and Interactions of Metavinculin.....59

4.3 Future Directions.....66

REFERENCES.....67

CURRICULUM VITAE.....77

LIST OF FIGURES

1.1 Ribbon diagram of full-length vinculin structure.....2

1.2 Basic components of an adherens junction.....5

1.3 Location of metavinculin insert in Vt and predicted structure.....8

1.4 Multiple sequence alignment of known metavinculin insert sequences.....9

2.1 Diagram of the pEB-T7 vector.....15

2.2 SDS-PAGE of all proteins purified.....16

2.3 Purification method of thioredoxin-fusion Vt/Mvt proteins.....19

3.1 CD melting curves of wild-type and mutant Mvt.....31

3.2 Mvt fragmentation with protease K.....32

3.3 ANS Emission spectra of CaM and Mvt.....33

3.4 Phenylsepharose elution profiles of Mvt and gradient analysis.....35

3.5 Competitive binding assay of Mvt to Vh.....37

3.6 Mvt-phospholipid cosedimentation assay.....38

3.7 PIP strip overlay assay.....40

3.8 Dimerization overlay assay.....41

3.9 Gel filtration of Vt and Mvt.....43

3.10 Mvt-actin cosedimentation assay.....44

3.11 Falling ball viscometry assay- Vt and/or Mvt in varying ratios with F-actin.....47

3.12 Falling ball viscometry assay- Vt/Mvt mixtures with increasing Mvt.....48

3.13 Vt straplock, armlock, and terminal-lock proteins.....49

3.14 EVH1 overlay assay.....50

3.15 SDS-PAGE and UV analysis of F5M-labelled NCys Proteins.....51

3.16 Permeabilized cells incubated with F5M-labelled NCys proteins.....53

4.1 Predicted Mvt insert structure and helical alignment.....55

LIST OF TABLES

2.1 Purified proteins and their experimental uses.....17

3.1 Percentages of Vt and Mvt pelleting with F-actin.....45

LIST OF ABBREVIATIONS

Amp-r – ampicillin resistance

ANS – 8-anilino-1-napthalenesulfonic acid

ATP – adenosine triphosphate

β-ME – β-mercaptoethanol

BCIP – bromo-4-chloro-3-indolyl phosphate

BSA – bovine serum albumin

CaM – calmodulin

CD – circular dichroism

CPM – 7-diethylamino-3-(4'maleimidylphenyl)-4-methylcoumarin

cps – counts per second

Ct1 – F-actin cosedimentation control

Ct2 – Vt or Mvt cosedimentation control

DCM – dilated cardiomyopathy

DEAE – diethylaminoethyl

DTT – dithiothreitol

ECM – extracellular matrix

EDTA – ethylenediaminetetraacetic acid

EGTA – ethylene glycol tetraacetic acid

EVH1 – Ena/VASP homology domain 1

F-actin – filamentous actin

F5M – fluorescein-5-maleimide

FAK – focal adhesion kinase

G-actin – monomeric actin

GST – glutathione-s-transferase

HIS – histidine

IPTG – isopropyl-β-D-1-thiogalactopyranoside

Kd – dissociation constant

kDa – kilodalton

Lac-Iq – lac repressor

LB – Luria-Bertani broth

Mvt – metavinculin tail, residues 877-1134

Mvt 833 – metavinculin tail, residues 833-1134

n – number of experiments

NBT – nitro blue tetrazolium chloride

NCys – N-terminal cysteine

P – pellet

PC – phosphatidylcholine

PDB – protein data bank

PI – phosphatidylinositol

PIP_2 – phosphatidylinositol-4,5-bisphosphate

PMSF - phenylmethanesulfonylfluoride

PS – phosphatidylserine

PtdIns(#)P – phosphatidylinositol-#-phosphate

S - supernatant

SD – standard deviation

SDS – sodium dodecyl sulfate

SDS-PAGE – SDS polyacrylamide gel electrophoresis

Std – protein standard

TB – terrific broth

TBS – Tris-buffered saline (20 mM Tris pH 7.5, 140 mM NaCl)

TBS-T – Tris-buffered saline + 0.1% Tween-20

TE – 10 mM Tris pH 8.0, 1 mM EDTA

TEM – 10 mM Tris pH 7.5, 1 mM EDTA, 5 mM β-ME

TEV – tobacco etch virus

T_m – melting temperature

TMN – 10 mM Tris pH 7.5, 5 mM β-ME, 250 mM NaCl

UV – ultraviolet

VASP – vasodilator-stimulated phosphoprotein

Vh – vinculin head, residues 1-835

Vt – vinculin tail, residues 877-1066

CHAPTER 1

INTRODUCTION

1.1 Overview

The ability of animal cells to connect with one another and with the extracellular matrix (ECM) is of critical importance for cell growth and motility, as well as the maintenance of cell integrity. Cells are connected to the ECM through integrin-mediated focal adhesions (Zamir and Geiger 2001), and to adjoining cells through cadherin-mediated adherens junctions (Perez-Moreno, Jamora and Fuchs 2003). Focal adhesions and adherens junctions are protein complexes which link cytoskeletal actin filaments to integrins and cadherins respectively. One protein of particular importance that is found in both of these junctions is called vinculin, which is derived from the latin word *vinculum*, meaning to link (Geiger 1979; Geiger, et al. 1980). Metavinculin, a splice variant of vinculin, is identical in sequence to vinculin with the exception of a 68 amino acid insert in its C-terminal domain (Strasser, et al. 1993), and shares most of the same ligands as vinculin, although its expression is restricted to muscular tissues (Belkin, et al. 1988; Witt, et al. 2004). Mutations within the metavinculin insert (Olson, et al. 2002; Vasile, et al. 2006) as well as a deficiency of metavinculin protein (Maeda, et al. 1997) have been associated with dilated cardiomyopathy.

1.2 Vinculin

1.2.1 Structure and Regulation

Vinculin is a 117 kDa, highly conserved, cytoskeletal protein of 1066 amino acid residues (Weller, et al. 1990) that localizes to focal adhesions and adherens junctions and is expressed in most human tissues (Ziegler, Liddington and Critchley 2006). The crystal

structures of full length chicken (Bakolitsa, et al. 2004), and human (Borgon, et al. 2004) vinculin have recently been solved and both show vinculin to be a globular, mostly helical protein with a 90 kDa N-terminal head domain (Vh)(residues 1-835), a proline-

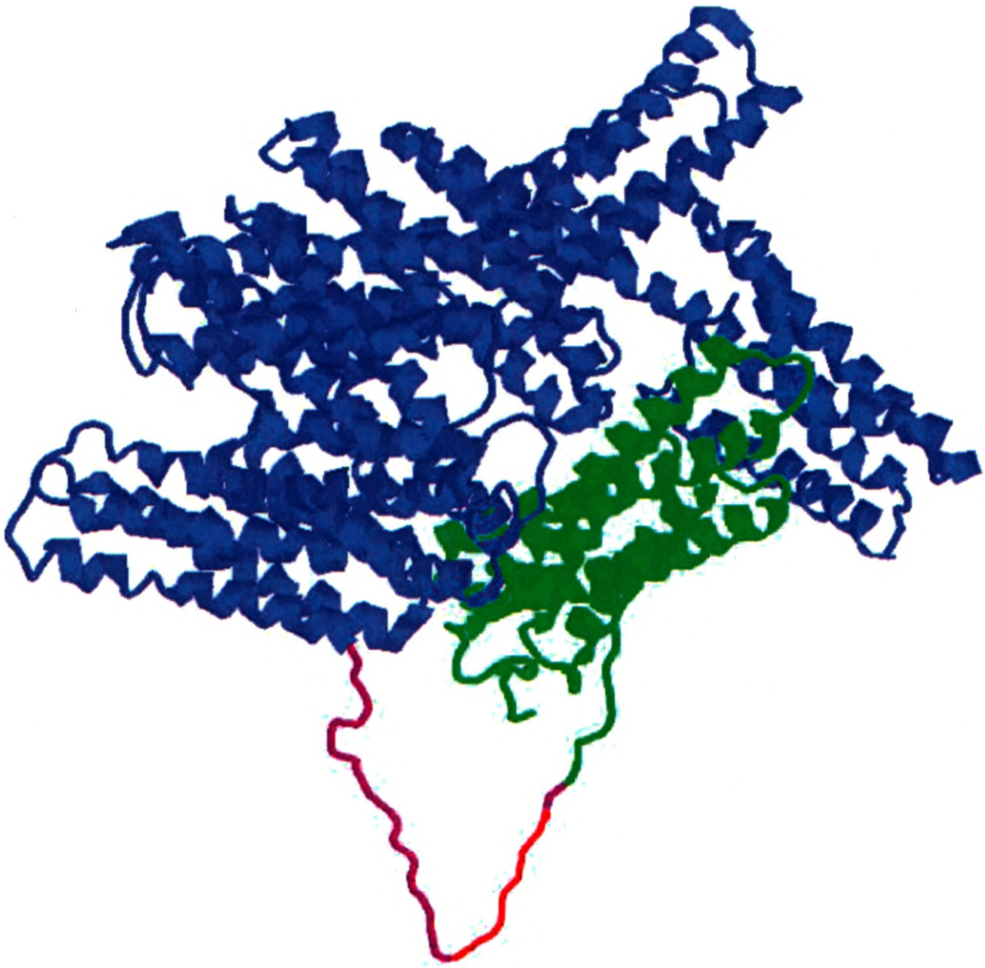

Fig. 1.1 Ribbon diagram of the crystal structure of autoinhibited full-length chicken vinculin (PDB ID: 1ST6) (Bakolitsa, et al. 2004). The Vh domain is depicted in blue, the Vt domain in green, and the hinge region in magenta. A portion of the hinge was not resolved in the crystal structure and was manually incorporated (shown in red).

rich hinge region (residues 836-876), and a 22 kDa C-terminal tail domain (Vt)(residues 877-1066) (Fig. 1.1). Vinculin is known to exist in at least two different conformations, depending on its binding partners. The crystal structures show vinculin in its closed, or autoinhibited conformation, in which the Vt domain is bound to two subsections of the Vh domain in a pincer-like arrangement. In the activated form of vinculin, the Vh and Vt domains dissociate and binding sites of many of their known ligands are exposed. The Vh domain has been shown to bind several proteins, including talin (Bass, et al. 2002; Izard, et al. 2004), α-actinin (Kroemker, et al. 1994), and α-catenin (Weiss, et al. 1998). Ligands of the hinge region include vasodilator stimulated phosphoprotein (VASP) (Brindle, et al. 1996), ponsin (Mandai, et al. 1999), vinexin (Kioka, et al. 1999), and Arp2/3 (DeMali, Barlow and Burridge 2002). The Vt domain binds F-actin (Huttelmaier, et al. 1997; Menkel, et al. 1994), paxillin (Wood, et al. 1994), protein kinase C-α (Weekes, Barry and Critchley 1996; Ziegler, et al. 2002), α-synemin (Sun, et al. 2008), raver1 (Huttelmaier, et al. 2001) and certain acidic phospholipids (Ito, et al. 1983)(Johnson and Craig 1995; Johnson, et al. 1998). Activation of autoinhibited vinculin has been proposed to occur as the result of the binding of one or more certain ligands, thus opening the molecule and allowing it to bind other ligands and form protein complexes. Some studies have suggested that vinculin may be activated through interaction with a single ligand, notably talin (Bois, et al. 2006; Izard, et al. 2004), α-actinin (Bois, et al. 2006), or PIP_2 (Gilmore and Burridge 1996). However, since the Vh-Vt interaction is of high affinity (Kd = ~ 1 nM) (Bakolitsa, et al. 2004), it has been theorized that the presence of a single ligand is insufficient to activate the molecule and that a combinatorial effect of two or more ligands is required (Janssen, et al. 2006).

Furthermore, the binding of acidic phospholipids and F-actin to vinculin have been shown to be mutually exclusive (Steimle, et al. 1999), since both of these ligands bind in a region of sequential exposed lysine and arginine residues that form a basic "ladder" within the third helix of the vinculin tail (Chandrasekar, et al. 2005; Janssen, et al. 2006). These two ligands separately are believed to expose cryptic dimerization sites within the Vt domain, allowing for oligomerization of vinculin and the subsequent cross-linking of actin filaments (Janssen, et al. 2006; Johnson and Craig 2000; Witt, et al. 2004).

1.2.2 Function

Vinculin was first discovered in 1979 by Geiger *et al.* as a contaminant during the purification of α-actinin, and was found to localize at the terminal ends of stress fibers within cultured cells (Geiger 1979; Geiger, et al. 1980). Vinculin has no known enzymatic function, but rather is believed to function as a scaffold protein and provide reinforcement at cell junctions (Gallant, Michael and Garcia 2005) through interactions with its many known ligands. The location of vinculin within the architecture of a simplified adherens-type cell junction model is shown in Figure 1.2. Since its initial discovery, the function of vinculin has been extensively studied using cultured cell and animal models.

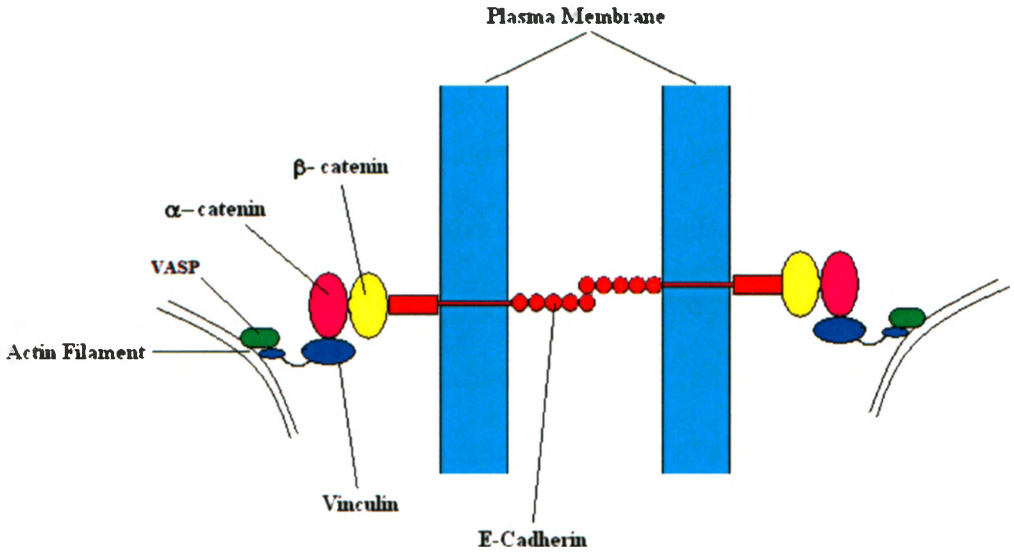

Fig. 1.2 Simplified model of an adherens junction between neighboring cells, adapted from Perez-Morena *et al.* (Perez-Moreno, Jamora and Fuchs 2003).

The mutation and subsequent reduced expression of vinculin in *Caenorhabditis elegans* resulted in muscle paralysis and L1 larval stage lethality, thus indicating that vinculin is essential for muscle function in nematodes (Barstead and Waterston 1991). Vinculin-null mice were found to be embryonic lethal beyond day E-10, with embryos 30-40% smaller in size relative to wild-type embryos and featuring underdeveloped limbs and sparse, fragile ectodermal tissue (Xu, Baribault and Adamson 1998). Furthermore, the cardiac and nervous systems of the embryos contained significant defects, thus indicating a potential role of vinculin in the development of these systems. In addition, heterozygous vinculin-knockout mice displayed normal development and basal cardiac function and histology, but had abnormal electrocardiograms and altered intercalated disc organization, which predisposed the mice to stress-induced cardiomyopathy (Zemljic-Harpf, et al. 2004). Thus, the importance of vinculin in embryonic development and at the cellular level of biological systems is evident.

It is interesting to note that cultured vinculin-null cells are still capable of forming focal adhesions, though complexes are smaller and less abundant relative to vinculin-positive cells (Volberg, et al. 1995). In addition, vinculin-null embryonic stem cells were found to have a round morphology relative to unaltered cells and displayed increased motility, decreased cell adhesion and spreading and rapid wound closure (Saunders, et al. 2006), yet were still able to differentiate into a variety of cell types found in early embryogenesis, thus indicating that vinculin is not required at this stage of development (Coll, et al. 1995). Overexpression of vinculin in cultured cells has also been evaluated, and resulted in the opposite effect of reduced cell locomotion and wound closure (Rodriguez Fernandez, et al. 1993). It is thought that vinculin regulates cell migration by stabilizing focal adhesions, and that interactions between vinculin and acidic phospholipids promote the dissociation of vinculin from such complexes, allowing for focal adhesion cycling (Chandrasekar, et al. 2005; Saunders, et al. 2006). Therefore, vinculin likely acts as a regulator of cell migration and spreading.

Vinculin has been implicated in the regulation of apoptosis and paxillin-focal adhesion kinase (FAK) signaling (Subauste, et al. 2004). Vinculin-null mouse F9 embryonic carcinoma cells displayed increased survival, up-regulation of the ERK1/2 proteins, and an increase in the paxillin-FAK complex. Paxillin is a ligand of the vinculin tail, and the paxillin-vinculin interaction is believed to regulate paxillin-FAK phosphorylation events (Subauste, et al. 2004). Finally, vinculin has been shown to have a role in tumor suppression. Vinculin levels were shown to be greatly reduced or undetectable in squamous cell tumors with metastatic potential, yet were normal in noninvasive basal cell tumors (Lifschitz-Mercer, et al. 1997). In addition, when vinculin

expression was restored in metastatic tumor cells and the cells were injected into mice, tumor formation in the mice was suppressed (Rodriguez Fernandez, et al. 1992).

1.3 Metavinculin

1.3.1 Sequence and Role

Metavinculin is a splice variant of vinculin which is identical in sequence to vinculin with the exception of an additional 68 amino acid insert present in the C-terminal tail domain (Fig. 1.3A) between the first and second helix (Fig. 1.3B). Metavinculin was first discovered in 1982 by Feramisco *et al.*, and was found to co-exist with vinculin in the dense bodies of smooth muscle tissue (Feramisco, et al. 1982). Tissue analyses have since determined that metavinculin is primarily expressed in smooth and cardiac muscle tissue (Belkin, et al. 1988) and has been shown to co-localize with vinculin (Belkin, et al. 1988; Feramisco, et al. 1982; Saga, et al. 1985) in certain muscular adhesive structures.

Although the structure of the insert remains unknown, the Garnier-Robson algorithm (Levin, Robson and Garnier 1986) predicts it to form three helical regions (Fig. 1.3C)(Olson, et al. 2002), the first two of which are acidic, and the third being basic. Alignment of the human, porcine, chicken, and frog metavinculin sequences revealed the C-terminal portion of the insert to be highly conserved, though the N-terminal portion somewhat variable in composition (Koteliansky, et al. 1992; Strasser, et al. 1993). An expanded version of this multiple sequence alignment is shown in Fig. 1.4, and further reveals a high degree of sequence similarity within the C-terminal half of the insert among all ten organisms shown. The N-terminal half of the insert was again found to vary not only in composition, but also in length, and thus the length of the insert ranges from

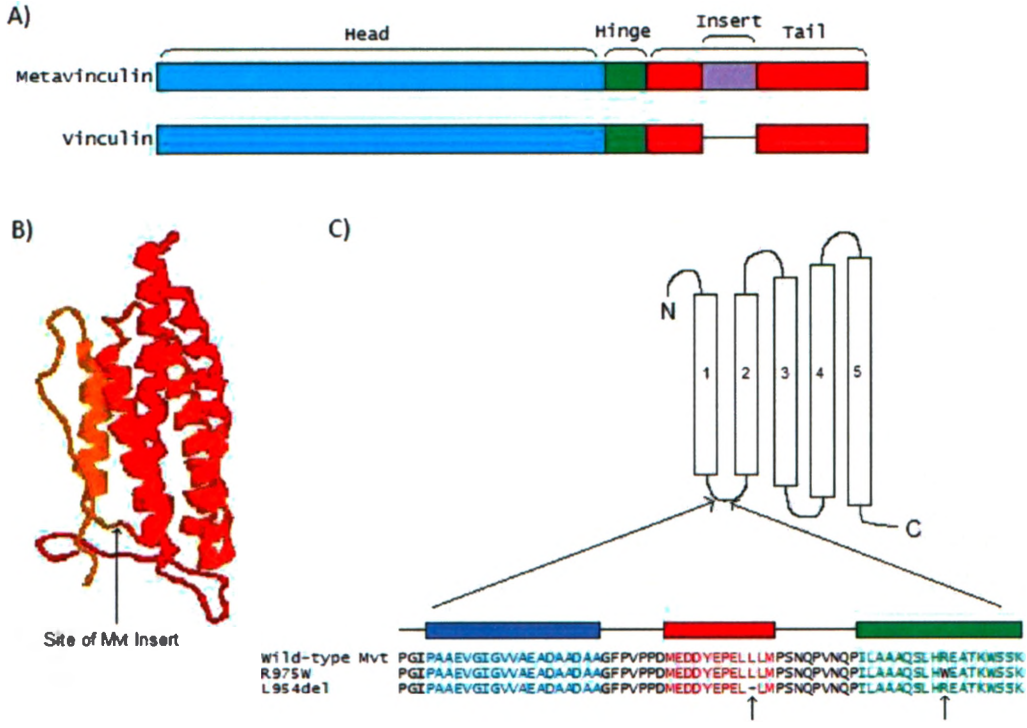

Fig. 1.3 A) Alignment of the domain structures of metavinculin and vinculin, with the metavinculin insert shown in purple. B) Cartoon representation of the vinculin tail, adapted from Bakolitsa *et al.* (PDB ID = 1ST6)(Bakolitsa, et al. 2004), with the location of the metavinculin insert indicated by the arrow. C) Diagram showing the location and predicted structure of the insert based on sequence analysis, adapted from Olson *et al.* (Olson, et al. 2002). The metavinculin insert is predicted to form three consecutive helices, depicted in blue, red, and green, respectively. The locations of the R975W and L954del mutations in the predicted structure are indicated with arrows.

64 residues in the zebrafish protein to 79 residues in that of the frog. The expression of metavinculin also appears to be confined to higher organisms. Although vinculin is known to be expressed in flies (Alatortsev, et al. 1997) and nematodes (Barstead and Waterston 1991), my analysis of their respective vinculin genes did not detect exons that encode the metavinculin insert, and thus these organisms do not express metavinculin isoforms.

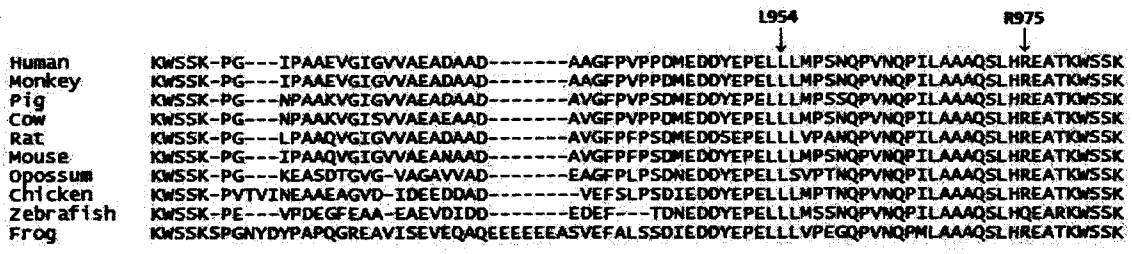

Fig. 1.4 Multiple sequence alignment of metavinculin proteins known to be expressed in selected species. The R975 and L954 residues of the human protein are indicated with arrows.

Metavinculin expression has been found to be highest in smooth muscle, and comprises about 35-42% of total vinculin present (Belkin, et al. 1988; Glukhova, et al. 1986). Measured relative amounts of metavinculin in cardiac muscle have been variable, ranging from trace amounts (Feramisco, et al. 1982) to approximately 20% of total vinculin (Belkin, et al. 1988). Small amounts of metavinculin have also been observed in skeletal muscle (Belkin, et al. 1988; Witt, et al. 2004), and human platelets (Turner and Burridge 1989). Metavinculin has been shown to localize at adherens junctions of the intercalated discs of cardiac muscle, which are specialized intercellular regions between adjacent cardiac myocytes. Intercalated discs contain several forms of cell-cell junctions, including a unique form of adherens junction known as the *fascia adherens*, which shares the same components as the *zonula adherens* of epithelial cells, but lacks its belt-like appearance (Fawcett and McNutt 1969). The nature of the various cell junctions within the intercalated discs allow for the low electrical resistance of these regions and for the transmission of force between adjoining cells as the heart muscle contracts (Perriard, Hirschy and Ehler 2003).

To date, no ligands specific to metavinculin have been discovered, but metavinculin has been shown to differ in affinity for certain ligands relative to vinculin.

With regard to intramolecular interactions, one group found the affinity of the metavinculin tail for the vinculin head to be approximately six times lower than that of the vinculin tail (Witt, et al. 2004), which might result in increased activation of the molecule. Also, metavinculin was found to have reduced affinity for acidic phospholipids relative to vinculin (possibly as the result of the overall negative charge of its insert), and this could result in reduced activation of the protein by acidic phospholipids (Witt, et al. 2004). Acidic phospholipids help expose cryptic dimerization sites of the tail domain, and the reduced affinity of metavinculin for phospholipids was found to result in reduced homodimerization as well as heterodimerization with vinculin (Witt, et al. 2004). However, vinculin incubated with acidic phospholipids was readily able to form heterodimers with metavinculin, and thus vinculin may be responsible for the activation or organization of metavinculin within focal adhesions and cell junctions. Metavinculin has also been shown to differ from vinculin in its organization of F-actin filaments (Olson, et al. 2002; Rudiger, et al. 1998), promoting the formation of dense filamentous networks as opposed to bundles. Metavinculin was also found to have a greater affinity than vinculin for the recently discovered raver1 protein (Huttelmaier, et al. 2001), which is believed to have a role in linking gene expression with functions of muscular contractile components (Zieseniss, et al. 2007). However, neither F-actin nor raver1 directly bind metavinculin within its insert, and thus it was predicted that the insert alters the conformation of metavinculin relative to vinculin. Furthermore, metavinculin appears to be more susceptible to phosphorylation than vinculin (Siliciano and Craig 1987), and this observation may be indicative of an important role in cell signalling. Since metavinculin reveals some differences in ligand interactions relative to vinculin and

shows restricted expression in specific tissues, it is probable that metavinculin serves a unique function that remains to be discovered.

1.3.2 Cardiomyopathic Mutations

Dilated cardiomyopathy (DCM) is a cardiac disease which is characterized by the impaired contraction and dilation of one or both ventricles (Richardson, et al. 1996). DCM has an incidence of 5-8 cases per 100 000 population and may affect all age groups, though most commonly individuals of middle age or older (Karkkainen and Peuhkurinen 2007). Although medical treatments for DCM have improved in recent years, cardiac transplantation is the only cure for the disease and DCM patients continue to have a high mortality rate (Olson, et al. 2002). The cause of DCM in some patients cannot be traced, and in these patients the disease is referred to as idiopathic DCM. In addition, environmental factors including viral infection and alcohol abuse are known to promote progression of DCM (Fatkin and Graham 2002). However, it is estimated that between thirty and fifty percent of DCM cases are caused by genetic mutations in certain cardiac proteins, including the β-myosin heavy chain, α-tropomyosin, cardiac actin, desmin, and dystrophin (Fatkin and Graham 2002).

Metavinculin was first linked to DCM in 1996 by Bowles *et al.* (Bowles, et al. 1996) when a familial inheritance of the disease was analyzed and a DCM-related locus was mapped to the chromosomal region where the metavinculin gene is located (10q21-23). It was since discovered that a mutation resulting in a loss of metavinculin was associated with the onset of DCM (Maeda, et al. 1997). In 2002, Olson *et al.* conducted a genetic screen on a group of DCM patients and discovered two separate point mutations within the metavinculin insert: one being a missense mutation (R975W), and the other a

three-base pair deletion (L954del) (Olson, et al. 2002). Pedigree analysis of the patient expressing the R975W mutation revealed that relatives expressing the mutation were also afflicted with the disease. Genetic information was not available from family members of the patient expressing the L954del mutation, though the patient's father and paternal uncle had both suffered from heart failure. The authors went on to examine the organization of actin filaments by wild-type and mutant forms of the metavinculin tail using falling-ball viscometry and fluorescent imaging. From the results it was concluded that wild-type metavinculin promoted the formation of filamentous actin networks, while the mutant forms induced the formation of actin bundles in a manner similar to vinculin. In addition, electron microscopy of cardiac tissue expressing the R975W mutant of metavinculin revealed an irregular and disordered appearance of intercalated discs. In a separate report, the R975W mutation has also been associated with hypertrophic cardiomyopathy (Vasile, et al. 2006), which is characterized by hypertrophy of one or both ventricles (Richardson, et al. 1996). Thus, the correlation of the metavinculin R975W mutation with two cardiac diseases and the association of the R975W and L954del mutations with familial incidences of dilated cardiomyopathy provide evidence that the mutations have a deleterious effect on the function of metavinculin.

The R975 and L954 residues were found to be highly conserved within known metavinculin sequences (Strasser, et al. 1993)(Fig. 1.4), which indicates that they might have an important role in the structure and/or function of the protein. In unaltered metavinculin, position 975 is located near the end of the third predicted helix (Fig. 1.3C), which is highly basic and thus has an overall positive charge. Mutation of a basic arginine residue to a large and hydrophobic tryptophan residue at this position might distort the

helix and/or disrupt inter-helical interactions as the overall positive charge of the third helix would be lessened. Position 954 is located near the end of the second predicted helix (Fig. 1.3C), and is the second of three consecutive leucine residues. Deletion of the leucine at position 954 will shorten the helix by one residue, and may also disrupt hydrophobic inter-helical packing. Thus, the mutations could have a structural effect or affect protein interactions.

1.4 Purpose of Thesis

The hypothesis behind this study is that cardiomyopathic mutations in metavinculin cause changes in protein and lipid binding properties relative to unmutated metavinculin and/or induce structural changes in the protein. Since it has been shown that a simple loss of metavinculin expression also causes the disease (Maeda, et al. 1997), mutation of these two highly conserved residues presumably has a deleterious effect on the function of the protein, rather than a gain-of-function. It has previously been reported that mutated metavinculin alters the organization of actin filaments (Olson, et al. 2002), providing a possible explanation for the onset of DCM, however, further characterization was warranted. The aim of this study was to evaluate structural differences between wild-type and mutant metavinculin, and to examine or re-examine differences in interactions between wild-type and mutant metavinculin and certain known ligands. Disease-causing mutations often identify critical functions in protein; therefore, changes in metavinculin properties due to these R975W and L954del mutations might lead to insights into its function. Because of both the ease of working with the metavinculin tail domain (as opposed to the complete protein) and its structural independence, the mutations were examined in the context of the tail.

CHAPTER 2

EXPERIMENTAL PROCEDURES

2.1 Cloning and Mutagenesis

DNA manipulation was conducted in accordance with standard procedures (Sambrook, Fritsch and Maniatis 1989). Analysis of gene sequences and restriction endonuclease cut sites was conducted using the computer software GENERUNNER (Hastings Software Inc., Hastings-on-Hudson, NY).

The R975W, L954del, and K944C mutations were previously incorporated into their appropriate genes by former members of the Ball lab. Wild-type and mutant Mvt, Vt, and Vh sequences were present in the pEB-T7 vector, a modified pET vector (Novagen, Madison, WI) which encodes an N-terminal thioredoxin fusion and tobacco etch virus protease cleavage site (Fig. 2.1). The EVH1 construct was incorporated into the pGEX-KG vector (Guan and Dixon 1991) by Sarah Aubut of the Ball lab.

2.1.1 N-terminal GST-fusion constructs

In order to express mutant Mvt as GST fusions, mutant Mvt sequences were digested from the pEB-T7 vector using *EcoRI* and *XhoI* cut sites and ligated into pGEX-KG, leading to a construct consisting of an N-terminal GST, a short linker sequence, and a C-terminal Mvt.

2.1.2 N-terminal cysteine constructs

An N-terminal cysteine (NCys) mutation (P878C) was previously incorporated into the Vt gene by Courtney Voss of the Ball Lab. To place this mutation into wild-type and mutant Mvt sequences, a three-way ligation was used. The NCys-Vt gene within the pEB-T7 vector was digested with the restriction enzymes *BglII* and *EarI*, giving rise to a

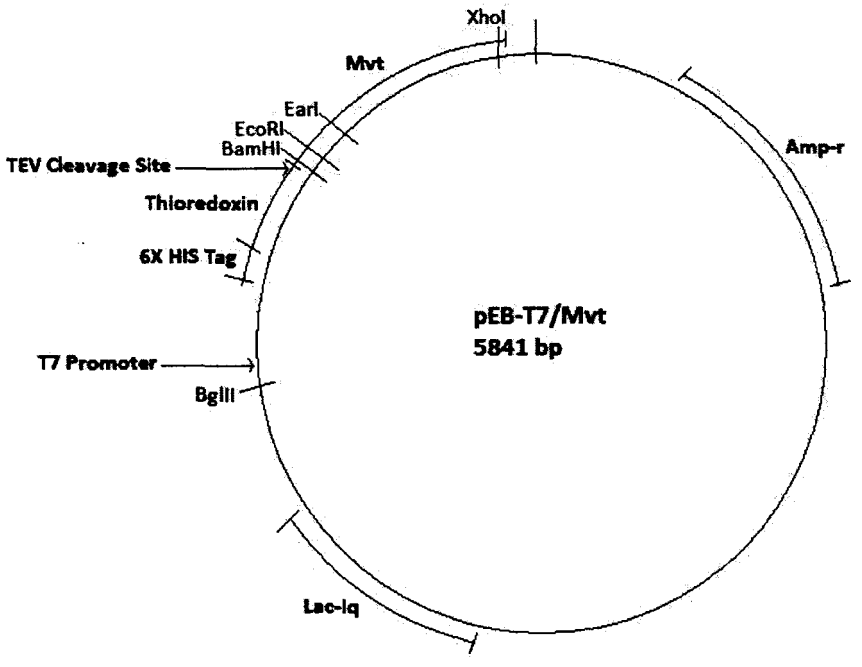

Fig. 2.1 Diagram of the pEB-T7 vector. Shown are important components of the vector and restriction enzyme sites that were used for cloning.

thioredoxin-containing fragment. The wild-type and mutant Mvt genes within the pEB-T7 vector were digested with the restriction enzymes *EarI* and *XhoI*, yielding a fragment encoding most of the Mvt sequence. These fragments were ligated into pCD, (a modified pCRBlunt vector) (Invitrogen, Carlsbad, CA) that was cut with *BamHI* and *XhoI* (the overhangs of *BamHI* and *BglII* being complementary). Once the ligations had correctly occurred, NCys-Mvt (wild-type and mutant) genes were excised using *BamHI* and *XhoI* and ligated into pEB-T7.

2.1.3 Mvt 833 constructs

A construct of Mvt 833 (residues 833-1134) was prepared in the pEB-T7 vector by Sarah Aubut of the Ball Lab. The L954del mutation was incorporated into the Mvt 833

gene via a three-way ligation into the pCD vector using the same restriction enzyme cut sites as were used in generating the N-terminal cysteine constructs. Using this protocol, the R975W mutation was incorporated into the Mvt 833 gene by Noha Albakri of the Ball Lab. Once the ligations had correctly occurred, mutant Mvt 833 genes were digested from pCD using *EcoRI* and *XhoI* and ligated into pEB-T7.

2.2 Protein Expression and Purification

Seventeen different proteins were purified in order to study the properties of wild-type and mutant metavinculin (Fig. 2.2). The experimental uses of these proteins are listed in Table 2.1, and the methods used in the purification of these proteins are outlined in this section.

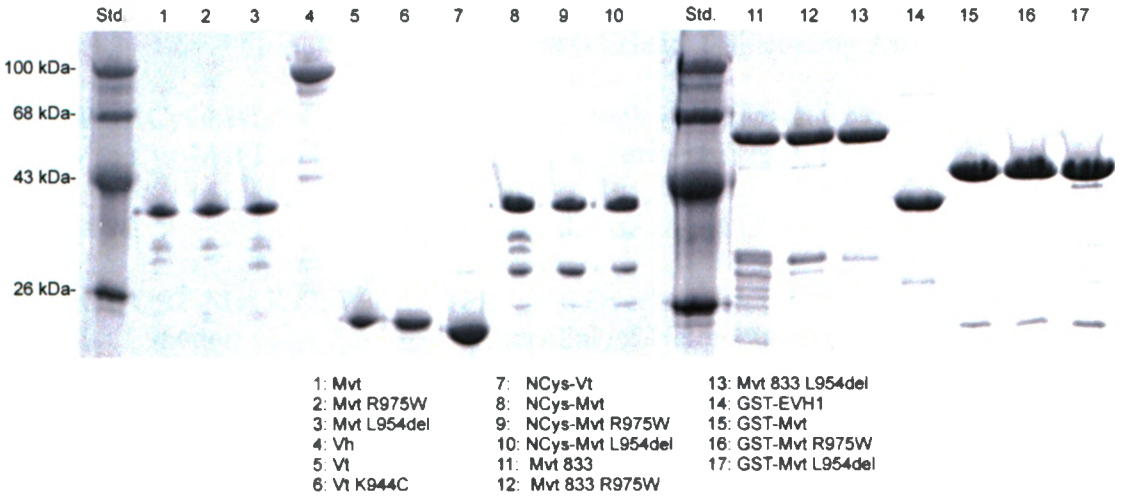

Fig. 2.2 SDS-PAGE of all proteins that were purified for experimental purposes.

Table 2.1 Purified proteins and their experimental uses.

Protein	Experimental Use
Mvt, Mvt R975W, Mvt L954del (residues 877-1134)	CD Melting Curves Protease K Proteolysis ANS Emission Spectra Phenylsepharose Binding Assay Fluorescent Head-Tail Binding Assay Lipid Cosedimentation Assay Actin Cosedimentation Assay Falling Ball Viscometry Nitrocellulose Heterodimerization Overlay Assay Gel Filtration (Mvt only)
Vh (residues 1-835)	Fluorescent Head-Tail Binding Assay
Vt (residues 877-1066)	Lipid Cosedimentation Assay Actin Cosedimentation Assay Falling Ball Viscometry Nitrocellulose Heterodimerization Overlay Assay Gel Filtration
Vt K944C	Labelling with Fluorescent Molecules Fluorescent Head-Tail Binding Assay
NCys-Vt, NCys-Mvt, NCys-Mvt R975W, NCys-Mvt L954del	Labelling with Fluorescent Molecules Binding to Permeabilized Cells
GST-EVH1	Nitrocellulose EVH1 Overlay Assay
GST-Mvt, GST-Mvt R975W, GST-Mvt L954del	PIP Strip Overlay Assay Nitrocellulose Heterodimerization Overlay Assay Western Blotting of Tissue Extracts (GST-Mvt only)
Mvt 833, Mvt 833 R975W, Mvt 833 L954del (residues 833-1134)	Nitrocellulose EVH1 Overlay Assay

2.2.1 Thioredoxin Fusions

Several colonies of *E.coli* strain BL21 containing the desired gene within the pEB-T7 vector were grown overnight at 37°C in 400 mL M9 media supplemented with 0.4% glucose, 0.2% casamino acids, and 100 μg/mL ampicillin. The following morning, the liquid culture was divided equally among four 1 L aliquots of LB media and

incubated at 37°C for two hours. Protein over-expression was induced by the addition of 0.2 mM IPTG and incubation at 22°C for five hours. Cultures were centrifuged at 2400 x g for ten minutes and cells resuspended in TE buffer (10 mM Tris pH 8.0, 1mM EDTA). Cells were lysed using either a French Pressure Cell (American Instrument Co., Silver Springs, MD) or an Emulsiflex-C3 Cell Homogenizer (Avestin Inc., Ottawa, ON) at 20 000 psi, then ultracentrifuged for one hour at 100 000 x g at 4°C to remove insoluble cellular debris.

2.2.1.1 Metavinculin/Vinculin Tail

The supernatant was passed through a 10 mL S-Sepharose column (GE Healthcare Life Sciences, Uppsala, Sweden) which was then washed with ten column volumes of TEM buffer (10 mM Tris pH 7.5, 1 mM EDTA, 5 mM β-ME) containing 10 mM NaCl. Protein was eluted from the column using TEM buffer supplemented with 250 mM NaCl. In preparation for NTA-Nickel column chromatography, fractions containing protein were combined and 10 mM imidazole and 2 mM $CaCl_2$ were added. These combined fractions were loaded onto a 5 mL NTA-Nickel column (Qiagen, Valencia, CA) and the column washed with TMN buffer (10 mM Tris pH 7.5, 5 mM β-ME, 250 mM NaCl) containing 10 mM imidazole. Protein was eluted from the column using TMN buffer supplemented with 250 mM imidazole. Protein-containing fractions were pooled, TEV protease was added to a final concentration of 20 μg/mg protein, and the protein dialyzed overnight at room temperature against TEM-50 (10 mM Tris pH 7.5, 1 mM EDTA, 5 mM β-ME, 50 mM NaCl). To further concentrate and purify the protein, it was loaded on to a 1 mL S-Sepharose column (GE Healthcare Life Sciences), washed, and eluted from the

column using TEM-250 buffer. The purification of NCys-Mvt is illustrated in Fig. 2.3 as an example.

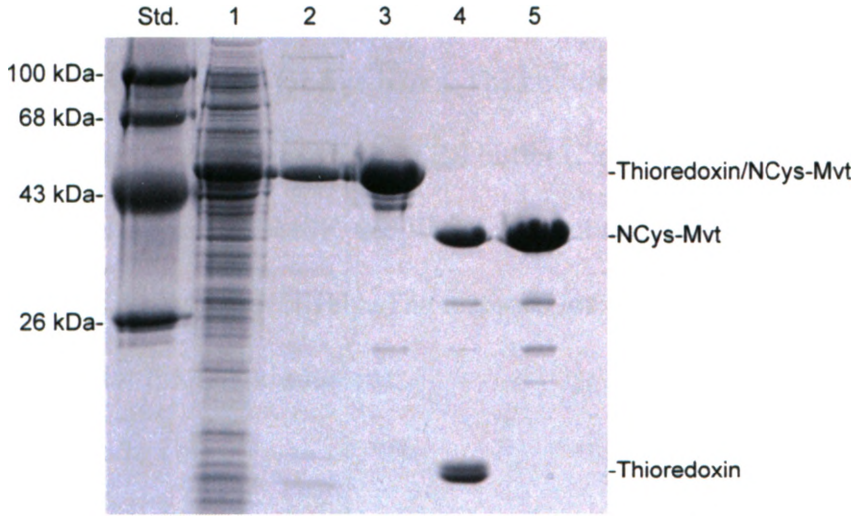

Fig. 2.3 Purification of NCys-Mvt expressed in the pEB-T7 vector. Lane 1: Cell lysate supernatant, Lane 2: after S-Sepharose column, Lane 3: after NTA-Nickel column, Lane 4: after TEV protease cleavage, Lane 5: final product.

2.2.1.2 Vinculin Head

Supernatant was passed through a 25 mL DEAE column (GE Healthcare Life Sciences) and the column washed with ten column volumes of TEM-50 buffer. Protein was eluted using TEM-300 (TEM buffer containing 300 mM NaCl). NTA-Nickel column chromatography, TEV protease cleavage, and dialysis were conducted as described for metavinculin/vinculin tail constructs. NTA-Nickel column chromatography was conducted a second time following TEV protease cleavage to remove the thioredoxin from the protein solution. Protein was concentrated using a 3 mL DEAE column (GE Healthcare Life Sciences).

2.2.2 GST-Fusions

A single colony of *E. coli* strain BL21 containing the desired gene within the pGEX-KG vector was grown overnight at 37°C in 800 mL TB media supplemented with 100 μg/mL ampicillin. Protein overexpression was induced with 0.2 mM IPTG and subsequent incubation at 22°C for five hours. The culture was centrifuged at 2400 x g for ten minutes and the pellet resuspended in TBS buffer (20 mM Tris, 140 mM NaCl) with protease inhibitors leupeptin, PMSF, and EDTA present at concentrations of 2 μg/mL, 0.035 mg/mL, and 1 mM, respectively. The methods for cell lysis and ultracentrifugation were the same as for thioredoxin fusions.

2.2.2.1 Metavinculin Tail

The supernatant was passed through a 10 mL glutathione-agarose column (Sigma, St. Louis, MO) and the column was washed with ten column volumes of TBS containing 5 mM β-ME and 1mM EDTA. Protein was eluted from the column with TBS containing 5 mM β-ME, 1mM EDTA, and 5 mM glutathione. Fractions of eluted protein were combined and diluted with TE buffer such that the NaCl concentration was reduced to 50 mM. These combined fractions were subsequently loaded on to a 3 mL S-Sepharose column (GE Healthcare Life Sciences) and the column washed with ten column volumes of TEM buffer containing 50 mM NaCl. Protein was eluted from the column with TEM buffer containing 250 mM NaCl.

2.2.2.2 EVH1 Domain

The cell lysate supernatant was subjected to glutathione-agarose column chromatography as described above. Fractions of eluted protein were combined and diluted with TE buffer such that the NaCl concentration was reduced to 50 mM.

Combined fractions were loaded on to a 3 mL DEAE column (GE Healthcare Life Sciences) and the column washed with ten column volumes of TEM-50 buffer. Protein was eluted from the column with TEM buffer containing 250 mM NaCl.

2.2.3 Labelling with Fluorescent Molecules

The Vt K944C protein was labelled with 7-diethylamino-3-(4'maleimidylphenyl)-4-methylcoumarin (CPM) (Invitrogen, Eugene, OR), and NCys (P878C) variants of Vt and Mvt were labelled with fluorescein-5-maleimide (F5M) (Invitrogen) using the same protocol. Stock solutions of each fluorescent label were prepared in dimethyl formamide to concentrations of 40 mM. A sample of 0.5 mL of 5 mg/mL of protein was treated with 2 mM DTT and incubated at room temperature for 30 minutes. A 10 mL P6DG gel column (Bio-Rad Laboratories, Hercules, CA) equilibrated with TEN-100 buffer (10 mM Tris pH 7.5, 1 mM EDTA, 100 mM NaCl), was used to desalt the protein and remove DTT. Protein was eluted and the absorbance at 280 nm measured. The protein fraction with the greatest protein content was incubated with 0.4 mM of label at room temperature in darkness for two hours and dialyzed overnight in TEN-50 buffer at 4°C. To further purify it, protein was loaded onto a 1 mL S-Sepharose column (GE Healthcare Life Sciences) and eluted with TEN-300 buffer.

2.3 Circular Dichroism Melting Curves

In preparation for circular dichroism spectropolarimetry, 3 mL of 0.3 mg/mL solutions of Mvt, Mvt R975W, and Mvt L954del were prepared and dialyzed against 10 mM KH_2PO_4 overnight. All data was collected using a Jasco J-810 CD Spectropolarimeter (Jasco Inc., Easton, MD) using a 0.4 mL amount of each protein solution in a quartz cuvette of path length 0.1 cm, in the presence of 1 mM DTT. A CD

spectrum was acquired for each protein over a wavelength range of 190 nm through 260 nm. Melting curves for each protein were generated in triplicate over a temperature range of 30°C through 95°C at a wavelength of 222 nm. The melting temperature of each protein was determined as the midpoint of the transition phase of each spectrum.

2.4 Protease K Proteolysis

Solutions of 0.5 mg/mL Mvt (wild-type and mutant) were prepared in the appropriate buffer (20 mM Tris pH 7.5, 100 mM NaCl, 1 mM EDTA) and 1 μg/mL Protease K (Ebeling, et al. 1974)(Qiagen, Valencia, CA) added to a final volume of 100 μL. Mixtures were incubated at room temperature with samples taken at 0, 10, 30, and 60 minutes and immediately treated with 1 mM PMSF. Samples were subjected to 15% SDS-PAGE.

2.5 ANS Emission Spectra

Prior to experimental trials, protein components were ultracentrifuged at 350 000 x g for 10 min to remove protein aggregates, and the buffer filtered using a 0.2 μm filter. Proteins (1 μM) were incubated with 100 μM 8-anilino-1-napthalenesulfonic acid (ANS)(Sigma) in 3 mL of buffer (20 mM Tris pH 8.0, 100 mM NaCl, 1 mM $CaCl_2$). Reactions were stirred in 4 mL acrylic cuvettes at constant temperatures (23°C or 37°C). Emission spectra were collected using a FluoroLog-3 Fluorimeter (Horiba Jobin Yvon, Edison, NJ) at an excitation wavelength of 380 nm.

2.6 Phenylsepharose Binding Assay

A 1 mL phenylsepharose (GE Healthcare Life Sciences) column was prepared in a glass Pasteur pipette. The column was washed with ten column volumes of wash buffer (10 mM Tris pH 7.5, 1M NaCl, 5 mM BME), 0.5 mg of protein was loaded onto the

column, and the wash was repeated. A gradient of decreasing NaCl concentration (1 M to 0 M) was generated in an acrylic gradient maker, and protein was eluted in 20-drop fractions. The conductivity of 200-fold dilutions of odd-numbered fractions was measured using a conductivity meter (Radiometer, Copenhagen, Denmark) and approximate NaCl concentrations in the fractions were determined using a standard plot of known conductivities. Protein in odd-numbered fractions was concentrated using trichloroacetic acid and sodium deoxycholate as described (Peterson 1977) and was resuspended in 30 μL Laemmli sample buffer (Laemmli 1970) before 12% SDS-PAGE. Relative amounts of protein in the fractions were evaluated by cutting bands from the resultant gels, and extracting and measuring the amounts of Coomassie Brilliant Blue (Ball 1986).

2.7 Fluorescent Head-Tail Competitive Binding Assay

The interactions between wild-type and mutant Mvt were examined using a fluorescent competition assay as described by Dr. Eric Ball (manuscript submitted). When CPM-Vt-K944C interacts with Vh, an increase in the fluorescent signal occurs, allowing calculation of the Kd via a non-linear regression fit to a binding model using the computer program DYNAFIT (Kuzmic 1996)(Biokin Ltd., Watertown, MA). When Mvt is included in the reaction, it acts as a competitor and its Kd can be determined by curve fitting to a competitive binding model using DYNAFIT. Experiments were conducted using a FluoroLog-3 Fluorimeter (Horiba Jobin Yvon) in TEN-100 buffer containing 0.02% TWEEN-20 and 100 μg/mL BSA at a constant temperature of 22°C. Excitation and emission wavelengths were 387 nm and 430 nm, respectively. A constant concentration of CPM-labelled Vt-K944C of 0.086 μM, and varying concentrations of

wild-type and mutant Mvt ranging from 0.35 μM to 0.95 μM were added to the reaction mixture. Prior to use, protein components were ultracentrifuged at 350 000 x g for 10 min to remove protein aggregates and the buffer subjected to 0.2 μm vacuum-filtration.

2.8 Lipid Cosedimentation Assays

Lipid cosedimentation assays were performed using a protocol similar to that described by Bakolitsa *et al.* (Bakolitsa, et al. 1999). Three sets of assays were conducted using either phosphatidylcholine (PC) (Avanti Polar Lipids, Alabaster AL), phosphatidylinositol (PI) (Sigma), or a mixture of 48% PC, 45% phosphatidylserine (PS), (Avanti), and 7% phosphatidylinositol 4,5 bisphosphate (PIP_2) (Avanti). Lipids were dissolved in chloroform to concentrations of 20 mg/mL and dried under nitrogen. Large multi-lamellar vesicles were prepared by hydrating the dried lipid in lipid buffer (20 mM Tris pH 7.5, 150 mM NaCl) at 42°C for 3 hours. Lipid mixtures were centrifuged at 16 000 x g at 4°C for 20 minutes and resuspended in the lipid buffer. Lipid-protein mixtures were prepared to a final volume of 0.1 mL with final lipid and protein concentrations of 0.5 mg/mL and 0.1 mg/mL, respectively, and incubated at 37°C for 30 minutes. Lipid-protein mixtures were ultracentrifuged at 140 000 x g for 10 minutes at 25°C and supernatants and pellets were separated and subjected to SDS-PAGE.

2.9 PIP Strip Overlay Assays

The binding of wild-type and mutant metavinculin to phospholipids was further analyzed using PIP Strips (Echelon Biosciences Inc., Salt Lake City, UT) using the protocol recommended by the manufacturer. All incubations were conducted in TBS-T buffer (20 mM Tris pH 8.0, 150 mM NaCl, 0.1% Tween-20) with 3% fatty-acid free BSA (Sigma) present. Between all incubations strips were washed three times with TBS-T

buffer for ten minutes. Strips were blocked for one hour using TBS-T with 3% BSA at room temperature, then incubated with GST-Vt, or wild-type or mutant GST-Mvt at concentrations of 500 ng/mL overnight at 4°C. Strips were subsequently incubated for one hour with 250 ng/mL monoclonal anti-GST antibody (WITS, London, ON) and then with 200 ng/mL alkaline phosphatase-labelled goat-anti-mouse IgG antibody (GE Healthcare Life Sciences) for one hour. Strips were each developed in 5 mL alkaline phosphatase buffer (100 mM Tris pH 9.5, 100 mM NaCl, 5 mM $MgCl_2$) using 1.65 mg/mL nitro blue tetrazolium chloride (NBT), and 0.825 mg/mL 5-bromo-4-chloro-3-indolyl phosphate (BCIP) for one hour.

2.10 Actin Cosedimentation Assays

Actin cosedimentation assays were conducted based on previously conducted protocols by Hemmings *et al.* (Hemmings, et al. 1996) and Janssen *et al.* (Janssen, et al. 2006). Mvt (wild-type or mutant) or Vt were diluted in actin polymerization buffer (10 mM Tris pH 7.5, 100 mM NaCl, 2 mM $MgCl_2$) either separately or in equimolar mixtures in amounts corresponding to 0.3, 0.6, or 0.9 molar ratios of total (meta)vinculin:actin to a final volume of 0.1 mL. G-actin from rabbit skeletal muscle (Cytoskeleton Inc., Denver, CO) was added to each reaction in 20 μg amounts and mixtures were incubated at room temperature for one hour. Mixtures were ultracentrifuged at 90 000 x g for one hour at 25°C, and supernatants and pellets subjected to SDS-PAGE.

2.11 Falling Ball Viscometry

Falling ball viscometry was conducted using a similar method to those described (MacLean-Fletcher and Pollard 1980; Pollard and Cooper 1982). The falling ball apparatus was previously calibrated by Courtney Voss of the Ball lab using glycerol

solutions at 20°C as described (Pollard and Cooper 1982). For each reaction, G-actin (Cytoskeleton) was added to actin polymerization buffer (10 mM Tris pH 7.5, 100 mM NaCl, 2 mM $MgCl_2$) to a final concentration of 0.3 mg/mL with either Vt or wild-type or mutant Mvt. 1 mM ATP was added to the reaction to a total volume of 400 µL and the actin solution was drawn into 100 µL glass capillaries (1.3 mm diameter, 12.7 cm in length)(Dade Diagnostics Inc., Miami, FL), upon which 4 cm distances had been clearly marked. The capillaries containing the actin solution were plugged at the bottom using adhesive putty and were incubated in a 25°C water bath for thirty minutes. Following the incubation, the capillary was placed on an angle of 50° in the same water bath, and a stainless steel ball (TRD Specialties Inc., Pine Meadow, CT) was placed in the entrance of the capillary and the time required for the ball to travel the 4 cm distance was measured.

2.12 Nitrocellulose Overlay Assays

Nitrocellulose overlay assays were conducted using wild-type and mutant Mvt and Mvt 833. Relevant proteins were spotted onto 1 x 10 cm strips of nitrocellulose in 1 µL amounts and allowed to dry for 15 minutes. All incubations were conducted at room temperature in TBS buffer (20 mM Tris pH 7.5, 140 mM NaCl) containing 5% skim milk. Between all incubations strips were washed two times with TBS buffer for ten minutes. Strips were initially blocked for two hours in TBS buffer/5% skim milk and subsequently incubated with 500 ng/mL of the appropriate GST-labelled protein for two hours. Strips were then incubated with 250 ng/mL monoclonal anti-GST antibody overnight. The following morning, strips were incubated with 200 ng/mL alkaline phosphatase-labelled goat-anti-mouse IgG antibody (GE Healthcare Life Sciences) for two hours. Strips were

developed in alkaline phosphatase buffer (100 mM Tris pH 9.5, 100 mM NaCl, 5 mM $MgCl_2$) using NBT and BCIP as described for the PIP strip overlay assay.

2.13 Gel Filtration

Solutions of 4 mg/mL protein were prepared using TEN-100 buffer with 0.5 mM DTT to volumes of 0.2 mL and ultracentrifuged at 350 000 x g for 10 min to remove protein aggregates. Samples of Vt, Mvt, and a mixture of both proteins were incubated at room temperature for 30 minutes. A 24 mL Superose 12 HR column (GE Healthcare Life Sciences) was connected to an AKTApurifier 100 (GE Healthcare Life Sciences) and the column was run at 0.5 mL/min using TEN-100 buffer with 0.5 mM DTT present.

2.14 Western Blotting of Tissue Extracts

Extracts of rat heart, brain, stomach, skeletal muscle, and liver tissues were previously prepared in Laemmli sample buffer (Laemmli 1970) by Dr. Ball. Samples of these extracts were subjected to 8% SDS-PAGE, and blotted to a nitrocellulose membrane at 100 V for one hour in Tris-Glycine buffer (25 mM Tris, 0.2 M glycine, 0.01% SDS) with 20% methanol (Towbin, Staehelin and Gordon 1979). The resultant membrane was stained with 1% amido black in 50% methanol and 10% glacial acetic acid for ten minutes. Guanidine treatment and renaturation of the blotted proteins was conducted using a similar method to those previously described (Ferrell and Martin 1989; Shackelford and Zivin 1993). The membrane was treated for one hour at room temperature in denaturation buffer (7M Guanidine-HCl, 50 mM Tris pH 7.5, 2mM EDTA, 1 mM DTT) and was subsequently washed twice for ten minutes using 30 mM Tris pH 7.5. Proteins were allowed to renature overnight 4°C in renaturation buffer (100 mM NaCl, 50 mM Tris pH 7.5, 2 mM DTT, 0.1 % Triton, 2 mM EDTA), with 5% skim

milk present to block the membrane. Blots were washed twice in 30 mM Tris pH 7.5, incubated with 0.5 μg/mL GST-Mvt for one hour in 1X TBS with 5% skim milk, and subsequently developed as described previously for the nitrocellulose overlay assays.

2.15 Binding of Metavinculin to Permeabilized Cells

Human cultured U2OS cells (human bone osteosarcoma) were cultured by Nicole St-Denis and Rich Derksen of Dr. David Litchfield's laboratory. The cells were plated in a 6-well, 35 mm tissue culture plate with 18 mm coverslips present at approximately 50 000 cells per well and were incubated at 37°C for three days. Fluorescein-labelled proteins were diluted in binding buffer (25 mM 2-[N-morpholino]ethane sulfonic acid (pH 6.0), 3 mM $MgCl_2$, 1 mM EGTA) to final concentrations of 100 μg/mL in total volumes of 80 μL. A 100-fold dilution of rhodamine-phallacidin (Sigma) was also included in the 80 μL aliquots. The binding of (meta)vinculin to permeabilized cultured U2OS cells was conducted as outlined by Ball *et al.* (Ball, Freitag and Gurofsky 1986). Mounted cells were viewed on a Zeiss Axiovert 25 inverted compound microscope and photographs were taken using an adjoining QICAM 10-bit camera (QImaging, Surrey, BC) and the Northern Eclipse computer software (Empix Imaging Inc., Mississauga, ON).

2.16 Other Techniques

SDS-PAGE was conducted using the Laemmli Buffer system (Laemmli 1970), the method of Lowry *et al.* (LOWRY, et al. 1951) as modified by Peterson (Peterson 1977) was used to determine protein concentration, and all protein molecular weights are expressed in kDa. The contrast of some photographs was linearly modified in figures displaying multiple images for the purpose of background matching.

The Lowry method of protein quantitation (LOWRY, et al. 1951; Peterson 1977) is known to be less variable than other protein determination protocols (Peterson 1983). To evaluate the reproducibility of this assay, the concentrations of twelve identical 2.4 μg samples of the same Mvt protein solution were measured and a 7% standard deviation resulted. Therefore, this protein determination method likely does not account for discrepancies in calculated protein concentration of greater than 7%.

CHAPTER 3

RESULTS

3.1 Physical Properties of Wild-Type and Mutant Metavinculin

The R975W and L954del mutations could potentially alter the structure of the metavinculin protein through disruption of weak interactions (eg. ionic and hydrophobic). Furthermore, since simply decreasing levels of metavinculin cause DCM, these mutations might simply reduce the stability of the protein. To examine the effects of these mutations on the structure and stability of metavinculin, wild-type and mutant Mvt were subjected to thermal denaturation, proteolysis, and hydrophobic surface assays.

To obtain the proteins, Mvt constructs present in the pEB-T7 vector were expressed and purified employing a combination of cation-exchange and affinity column chromatography. This purification method produced yields of about 5 mg protein/L of cell culture, and there did not appear to be any large differences in yield among wild-type Vt, Mvt, or any of their modified forms. SDS-PAGE analysis indicated that none of the proteins revealed large amounts of degradation between cell lysis and concentrating ion-exchange column chromatography, and purities of concentrated protein solutions greater than 85% were obtained (see Fig. 2.2).

To examine differences in thermal stability between wild-type metavinculin and its R975W and L954del mutants, samples of Mvt, Mvt R975W, and Mvt L954del were subjected to circular dichroism (CD) spectropolarimetry (Fig. 3.1). The melting temperature (T_m) of each protein was measured as the midpoint of the transition phase of the melting curve. The curves were of a similar sigmoidal shape, showing gradual

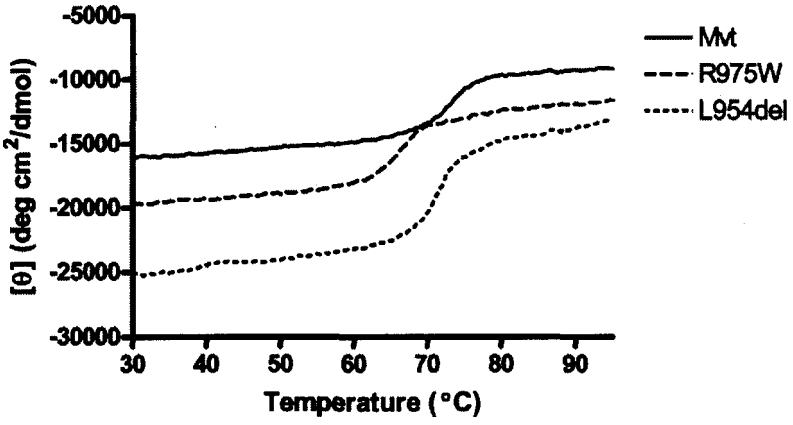

Fig. 3.1 Circular Dichroism melting curves of wild-type and mutant Mvt measured at 222 nm over a temperature range of 30°C though 95°C.

increases in signal ellipticity (θ) with increasing temperature, and a transitional period in which the ellipticity rises sharply in correspondence with thermal denaturation of the proteins. Although the curves were similar in shape, their degrees of ellipticity were found to differ. CD measurements are highly sensitive to protein concentration (Hennessey and Johnson 1982), and slight over- or underestimations of protein concentrations may have led to this observation. The average melting temperatures (+/- SD) of Mvt, Mvt R975W, and Mvt L954del (n = 3) were determined to be 72.0 +/- 0.5°C, 66.1 +/-0.3°C, and 71.3 +/- 0.2°C. The melting temperature of Mvt R975W was found to be significantly lower than that of Mvt ($P < 0.05$), while the melting temperature of Mvt L954del was not. The R975W mutation may alter the structure of Mvt, or this mutation may increase the stability of the denatured form of the protein.

Possible differences in structure among wild-type and mutant Mvt were further analyzed by limited proteolysis with protease K, which cleaves peptides C-terminal to hydrophobic aliphatic and aromatic amino acids (Ebeling, et al. 1974). After protease

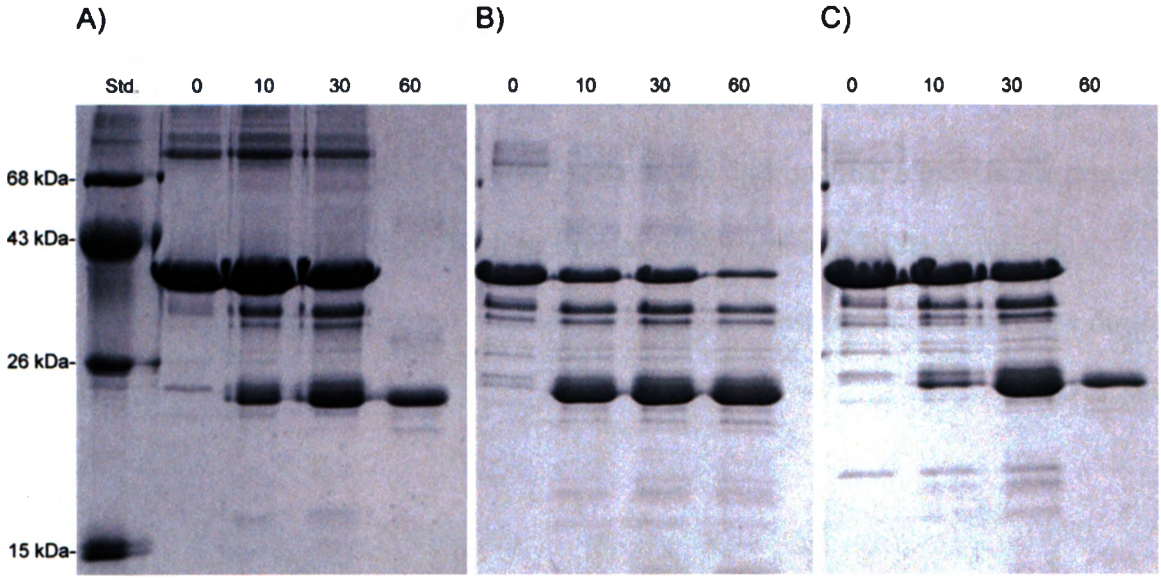

Fig. 3.2 15% SDS Gel analysis of the proteolysis of A) Mvt, B) Mvt R975W, and C) Mvt L954del with Protease K, after 0, 10, 30, and 60 minutes of degradation.

addition, samples were taken at various times and fragmentation patterns analyzed using SDS-PAGE (Fig. 3.2). In each case, the majority of the full-length Mvt was degraded after 60 minutes, yielding a stable fragment of approximately 22 kDa. The band patterns were very similar, although the rate of degradation of the Mvt R975W protein appeared to be slightly slower in this experiment. Overall, the data provide evidence that the R975W and L954del mutations do not induce large conformational changes in Mvt.

Mutations that alter the protein structure might be expected to lead to greater exposure of hydrophobic surface. To investigate this possibility, the exposed hydrophobic surfaces of wild-type and mutant Mvt were evaluated using the fluorescent probe 8-anilino-1-napthalenesulfonic acid (ANS), which emits a strong fluorescent signal in a hydrophobic environment (Saucier, et al. 1985; Stryer 1965). Emission spectra from 1 μM of each protein were collected in the presence of a 100-fold excess of ANS over a range of 400 - 600 nm. In all cases, the buffer emitted a small raman peak at

approximately 435 nm (Fig. 3.3). For comparative purposes, spectra of calmodulin (CaM) were conducted in the presence and absence of calcium (Fig. 3.3A) (LaPorte, Wierman and Storm 1980; Steiner 1984). CaM exposes a highly hydrophobic region in the presence of calcium, as is indicated by the high maximum of its spectra (~5-fold increase in intensity) and the shift of the maximum to 480 nm. In the absence of calcium CaM does

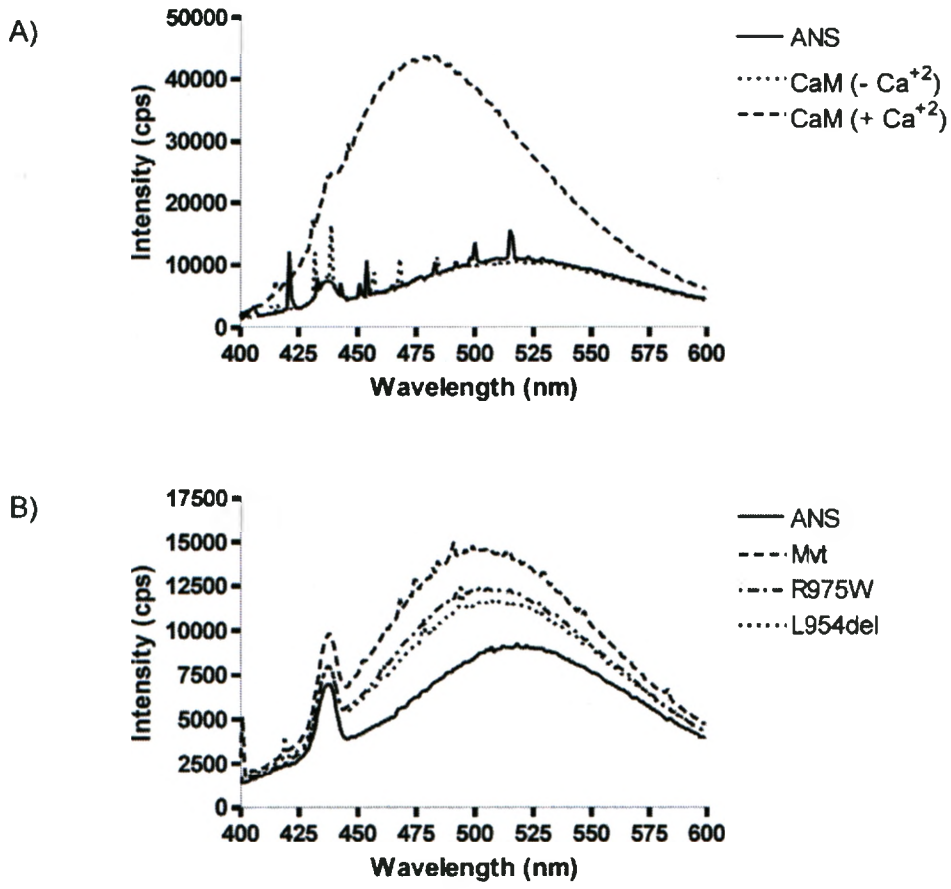

Fig. 3.3 A) Emission spectra of 100 μM ANS and 1μM CaM in the presence and absence of calcium. B) Spectra of ANS with 1 μM Mvt, Mvt R975W, and Mvt L954del at 23°C.

not expose this region and has a highly polar surface, indicated by the lack of change in the emission of ANS alone (Fig. 3.3A). Contrary to expectations, wild-type Mvt yielded a greater peak upon interaction with ANS than either of the mutants, both of which produced similar spectra (Fig. 3.3B). Furthermore, the spectra of all three proteins yielded maxima that were only slightly greater than that of ANS alone (and much less than that of CaM with Ca^{+2}), indicating that the surfaces of the proteins are largely hydrophilic. Since hydrophobic forces increase with temperature, the experiments were repeated at 37°C but yielded very similar results (not shown). Thus, these results suggest that the structure of unmutated Mvt displays a slightly greater degree of hydrophobic surface area than the mutants.

Since a possible difference in exposed hydrophobic surface was detected among wild-type and mutant Mvt, the binding of wild-type and mutant Mvt to phenylsepharose was examined as a different method to further investigate their surface hydrophobicity. After binding to a phenylsepharose column under conditions of high salinity, Mvt was eluted from the column with a decreasing salt gradient. The Mvt content of odd-numbered fractions was evaluated using SDS-PAGE (Fig. 3.4A), and was subsequently quantified (Fig. 3.4B). Both the SDS gel analysis and absorbance measurements indicate a similar elution profile for Mvt and its R975W and L954del mutants, with a gradual increase in eluted protein beginning at around fraction 9 and peaking at fraction 23. The salt gradient was checked by conductivity measurements of the fractions and did not differ among the three proteins (Fig. 3.4C). Since the elution profiles of the proteins are similar, by this criterion wild-type and mutant Mvt have very similar amounts of exposed hydrophobic surface.

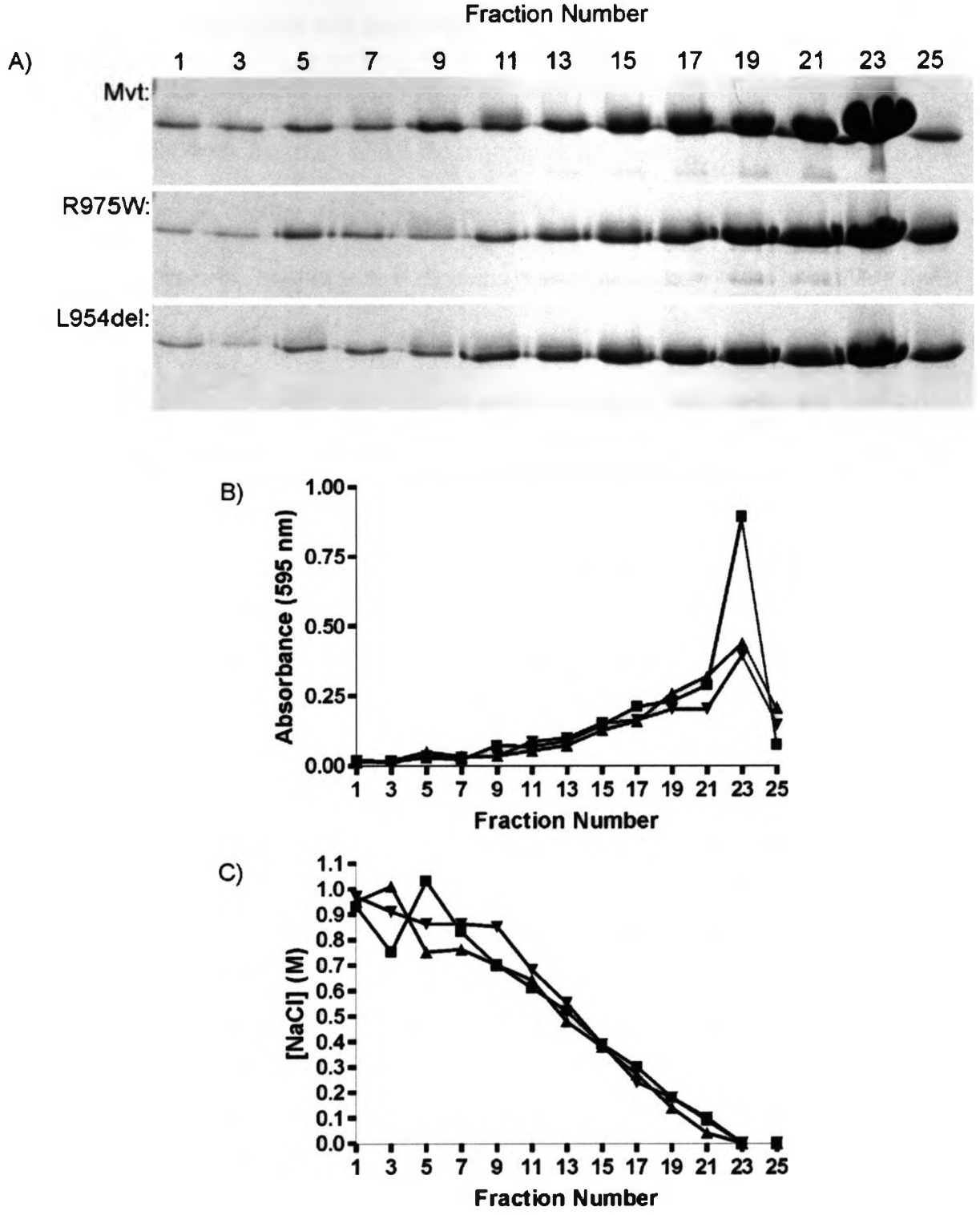

Fig. 3.4 A) SDS-PAGE of odd-numbered fractions eluted from a phenylsepharose with decreasing salinity. B) Quantitation of Mvt (■), Mvt R975W (▲), and Mvt L954del (▼) detected on the SDS gels shown in (A). Bands were cut from the gels, the Coomassie brilliant blue dye extracted, and the resulting absorbances measured. C) The decreasing NaCl gradient for the elution of each protein.

3.3 Biological Properties and Interactions of Metavinculin

Since the mutations did not appear to cause large structural alterations in Mvt, another possibility is that they affect the binding characteristics of Mvt with its known ligands. An intramolecular interaction between Mvt and Vh occurs in the autoinhibited form of metavinculin, and these two domains must dissociate in order to activate the protein and expose many of its ligand binding sites. To examine whether the R975W and L954del mutations affect the activation of metavinculin, the intramolecular interaction between wild-type or mutant Mvt and Vh was examined using a fluorescent competitive binding assay. The Vt-K944C mutation occurs near the binding site for Vh and thus when labelled with a fluorescent coumarin-maleimide molecule (CPM), fluorescent changes occur upon the Vt-Vh interaction. Competition by unlabelled Mvt or Vt decreases these changes in the fluorescent signal, and this information can be used to estimate the dissociation constant (Kd) between the inhibitor and Vh (Fig. 3.5A). The average Kd for the binding of CPM-Vt-K944C to Vh was found to be 1.8 μM ($n = 3$). The average Kd values (+/- SD) for the binding of Mvt, Mvt R975W, and Mvt L954del to Vh ($n = 4$) were determined to be 37.7 +/- 8.0 nM, 48.1 +/- 4.8 nM, and 75.9 +/- 37.9 nM, respectively (Fig. 3.5B). The Kd values of the mutants were not significantly different from that of the wild-type ($P > 0.05$), and thus the R975W and L954del mutations do not appear to change the intramolecular interaction between Mvt and Vh.

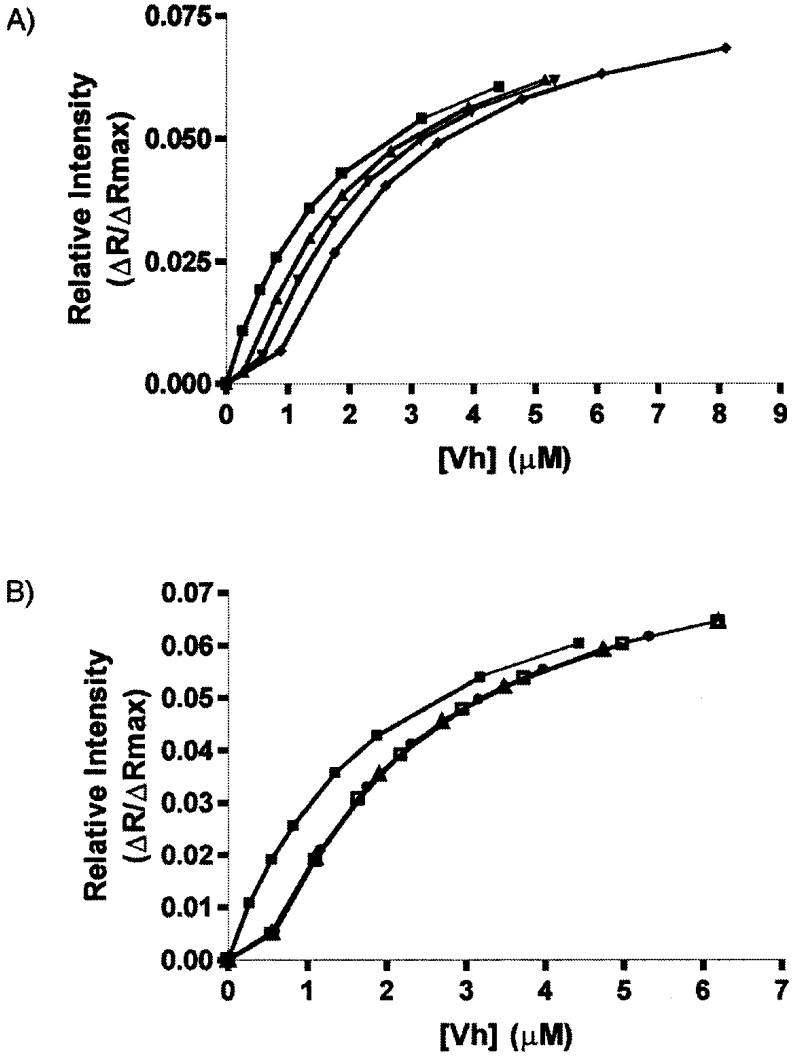

Fig. 3.5 A) Binding of CPM-labelled Vt-K944C to Vh in the absence (■) and presence of increasing amounts (0.35 μM (▲), 0.59 μM (▼), 0.95 μM (◆) of wild-type Mvt. B) Inhibition of the CPM-Vt-K944C-Vh interaction (■) by similar concentrations of Mvt (●), Mvt R975W (□), and Mvt L954del (Δ).

The interaction of Vt and Mvt with certain acidic phospholipids has been established and may be important in focal adhesion regulation (Chandrasekar, et al. 2005; Saunders, et al. 2006). Therefore, differences in affinity of wild-type and mutant Mvt for acidic phospholipids were analyzed using cosedimentation assays. Proteins in the

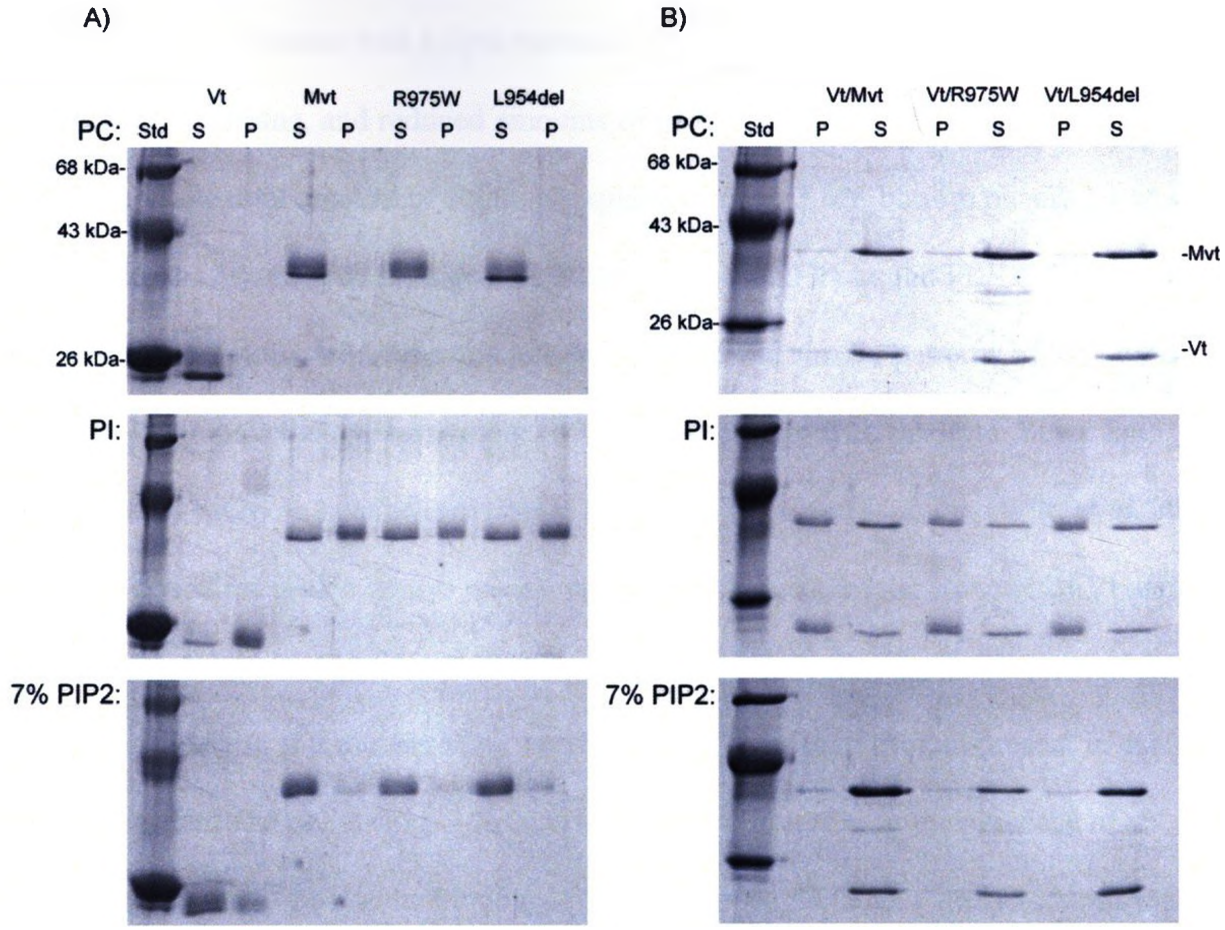

Fig. 3.6 SDS-PAGE of pellets (P) and supernatants (S) resulting from the cosedimentation of Vt and Mvt with phospholipids. Cosedimentations were conducted A) with Vt and Mvt separately and B) in equimolar mixtures. Note that S and P lanes are reversed in A) and B).

supernatant and lipid pellet were subsequently analyzed using SDS-PAGE (Fig. 3.6A). Vinculin has previously been found not to bind the neutral phospholipid PC (Ito, et al. 1983), and therefore this lipid was used as a control. Cosedimentation of the proteins with this neutral lipid confirmed the previous observation, as all protein appeared in the supernatant (Fig 3.6A, top panel). Vt showed a greater affinity for PI than Mvt, as was evident since a greater proportion of Vt pelleted with PI than Mvt (80% versus 50%). Furthermore, the mutant Mvt proteins behaved in a similar manner to the wild-type as was evident by their similar banding patterns on the gels (Fig. 3.6A, middle panel).

Proteins were incubated with a lipid mixture containing 7% PIP_2, used as a closer analog to the cell membrane, and reduced amounts of protein were pelleted as a result of the decrease in the total amount of acidic phospholipid (Fig. 3.6A, bottom panel). However, as was demonstrated with PI, a greater proportion of total Vt bound PIP_2 (~25%) relative to Mvt. Furthermore, wild-type and mutant Mvt showed similar patterns of PIP_2 binding, each of which pelleted approximately 15% of total protein with the lipid. Since lipid binding may promote heterodimerization of metavinculin and vinculin (Witt, et al. 2004), the lipid cosedimentation assays were repeated using an equimolar mixture of Vt and Mvt (Fig. 3.6B). When incubated with PI, there did not appear to be any difference in binding between wild-type and mutant Mvt, with roughly 50% of total protein present in each of the supernatant and pellet (Fig. 3.6B, middle panel). However, in the presence of an equimolar amount of Mvt, the binding of Vt to PI appeared to be slightly reduced relative to its separate cosedimentation, with approximately 60% of total protein present in the pellet (Fig. 3.6B, middle panel). When the protein mixtures were cosedimented with 7% PIP_2, the affinities of all four proteins for PIP_2 appeared to be similar, although less than 10% of total protein pelleted with the lipid in each case (Fig. 3.6B, bottom panel). The specificity of wild-type and mutant Mvt and Vt for different phospholipids was evaluated using PIP strips. PIP strips were incubated with GST-Vt purified by a former member of the Ball Lab) or GST-Mvt and lipid-protein interactions were detected using anti-GST and an alkaline-phosphatase color reaction. GST-Vt showed weak interaction with lipids spotted on the PIP strips, indicated by the faint staining pattern as compared to that of the

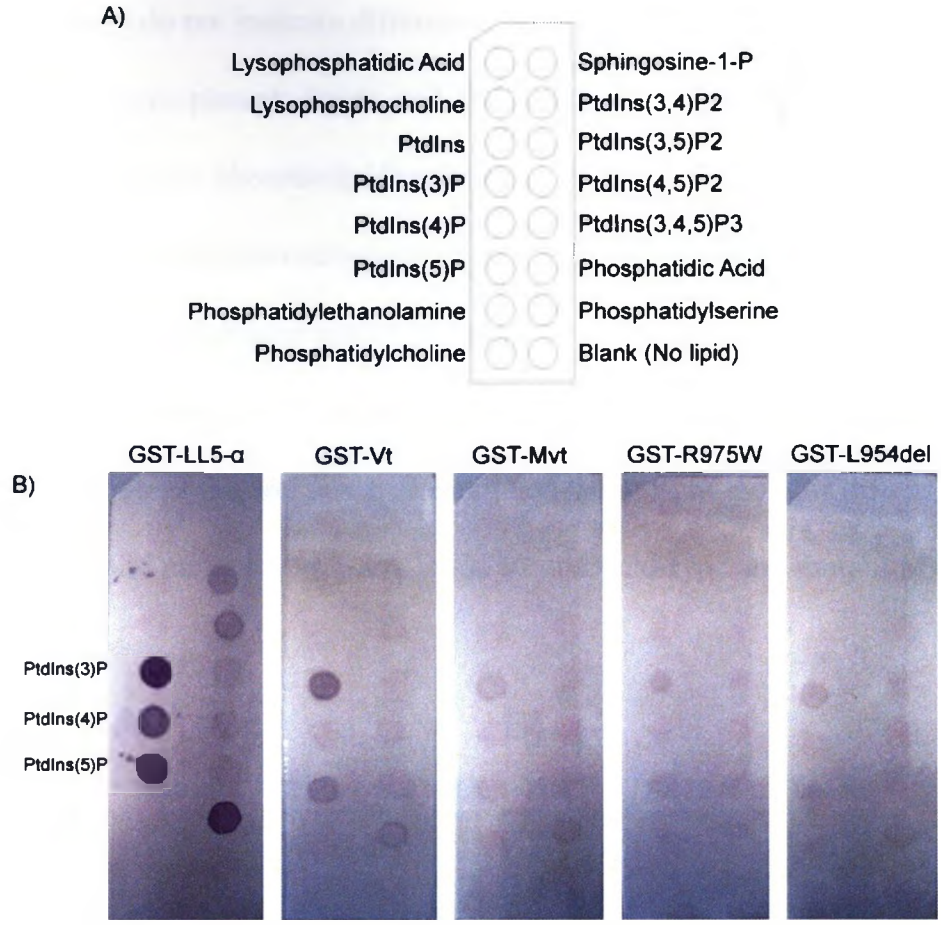

Fig. 3.7 PIP strip overlay assays with GST-labelled Vt and Mvt. A) The lipid spotting order of the PIP strips as indicated by the manufacturer. B) Photographs of the PIP strips following incubation and development.

LL5-α pleckstrin homology domain (a manufacturer-supplied positive control), and GST-Mvt interactions were weaker still (Fig. 3.7). In each case, the most clearly visible staining occurred at PtdIns(3)P and PtdIns(5)P spots, indicating an apparent specificity of Vt and Mvt for these lipids relative to PtdIns (PI) and other phosphorylated PI variants . Only trace amounts (not clearly resolved in the photographs) were detected at spots corresponding to these and other acidic phospholipids (Fig. 3.7). There were no apparent differences in either staining patterns or intensity among strips incubated with GST-Mvt, GST-Mvt R975W, and GST-Mvt L954del. The results of the cosedimentation and PIP

strip binding assays do not indicate differences in affinity among Mvt, Mvt R975W, or Mvt L954del for acidic phospholipids, and confirms the previously reported reduced affinity of Mvt for acidic phospholipids relative to Vt (Witt, et al. 2004).

Homo- and heterodimerization of Vt and/or Mvt has been suggested to occur upon interaction with either F-actin or acidic phospholipids (Janssen, et al. 2006; Witt, et al. 2004). Since dimerization may be important for the function of (meta)vinculin, lipid-induced dimerization of the proteins was examined using PI to look for differences among wild-type and mutant Mvt. Samples of Vt and wild-type and mutant Mvt were

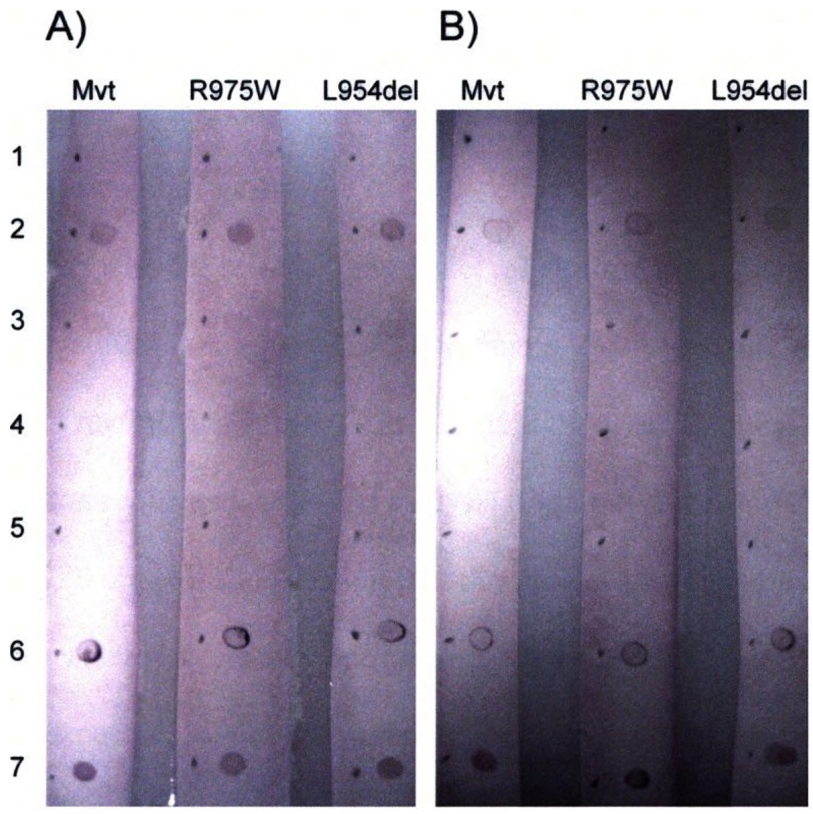

Fig. 3.8 Nitrocellulose overlay assays examining homo- and heterodimerization of Vt and Mvt in the presence and absence of PI. Strips were probed with A) GST-Vt and B) GST-Mvt, GST-Mvt R975W, and GST-L954del. Spotting order is as follows: 1) 1 μg BSA, 2) 0.02 μg GST, 3) 1 μg PI, 4) and 5) 1 μg of Vt and Mvt respectively (wild-type or mutant) without PI, 6) and 7) 1 μg of Vt and Mvt respectively (wild-type or mutant) with PI present.

incubated with a 10-fold molar excess of PI. Nitrocellulose overlay assays were conducted in which Vt and Mvt (both with and without PI) were spotted on to nitrocellulose strips before probing with GST-Vt or GST-Mvt. Following immunodetection, there were no apparent interactions among Vt and/or Mvt in the absence of lipid, but homo- and heterodimerization were detected among proteins that were pre-incubated with PI (Fig. 3.8). The strips yielded similar degrees of staining at the GST positive control (spot #2). On each strip, Vt/PI resulted in predominant staining around the periphery of the spot (spot #6), contrary to Mvt/PI which produced more uniform staining (spot #7) in a similar manner to that of the GST control. There did not appear to be any differences in homo-or heterodimerization of wild-type and mutant Mvt as was evident by their similar degrees of spot intensity. In all cases, staining was more intense than that of PI alone (spot #3).

To determine whether soluble Vt and Mvt might form heterodimers, these proteins were subjected to gel filtration analysis. Vt, Mvt, and a Vt-Mvt mixture were prepared to concentrations of 4 mg/mL and subjected to gel filtration under identical conditions with twenty 1 mL fractions collected. SDS-Gel analysis (Fig. 3.9) and absorbance measurements at 280 nm (not shown) indicated that Vt and Mvt eluted in approximately the same fractions when run separately or together, suggesting little tendency to form heterodimers. As expected, Mvt eluted in earlier fractions than Vt because of its higher molecular weight. Protein complexes of greater molecular weight than Mvt were not detected in fractions that were eluted earlier than Mvt, providing further evidence that dimer complexes were not stable under these conditions.

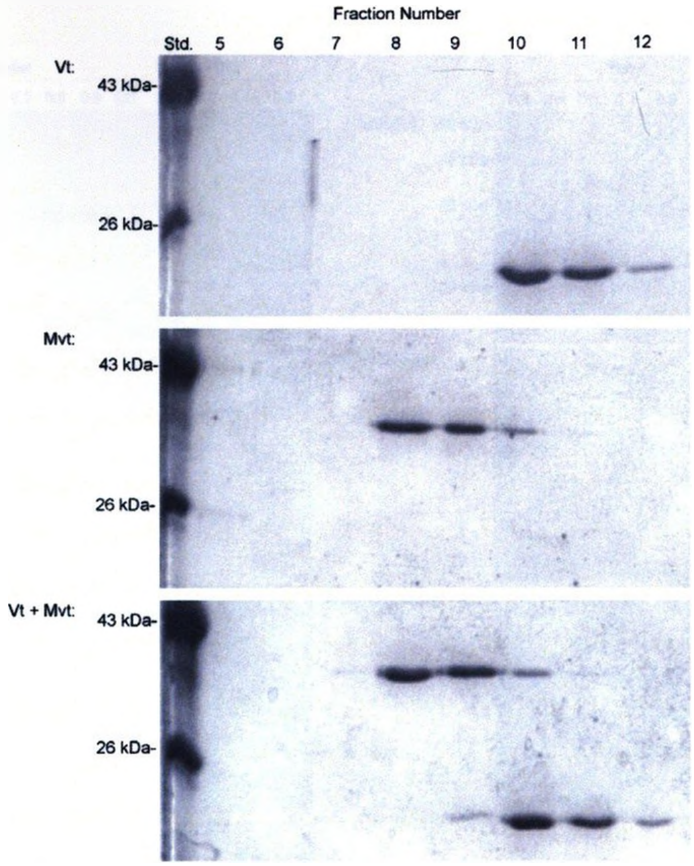

Fig. 3.9 Gel filtration of Vt, Mvt, and a Vt-Mvt mixture on a 24 mL Superose-12 HR column. Fractions 5-12 from each elution were subjected to SDS-PAGE.

The metavinculin tail has been shown to bind filamentous actin, and a previous study suggested that the metavinculin R975W and L954del mutations alter actin organization (Olson, et al. 2002). In an effort to confirm and extend these observations, Mvt interactions with F-actin were examined further. Cosedimentation assays were conducted to examine the affinity of metavinculin for F-actin. Vt and Mvt were incubated with F-actin in several molar ratios, then ultracentrifuged before SDS-PAGE (Fig. 3.10A). For each trial a majority of actin was pelleted, though trace amounts

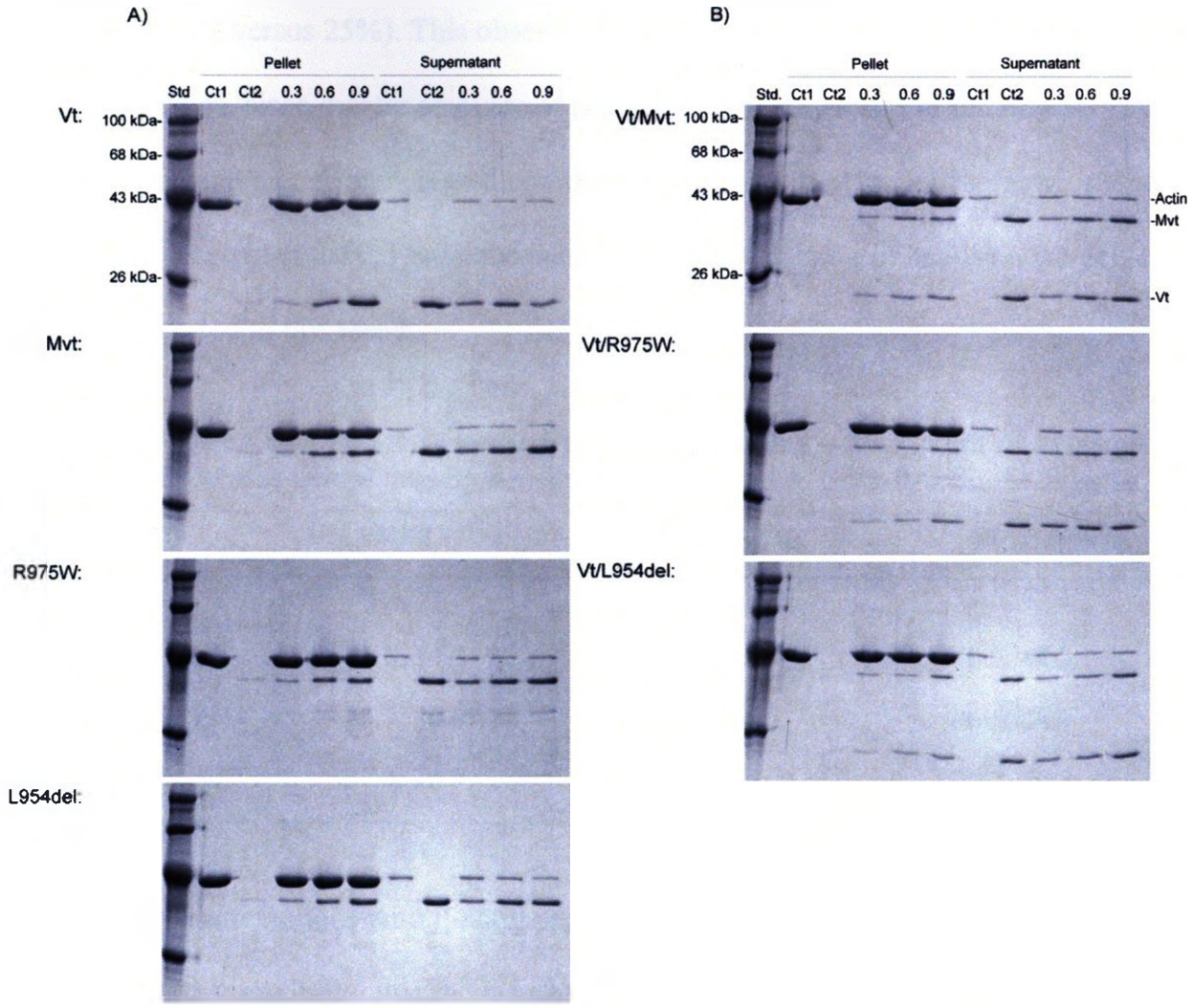

Fig. 3.10 Cosedimentation of Vt and Mvt with F-actin in 0.3, 0.6, and 0.9 molar ratios (meta)vinculin:actin. As controls, F-actin (Ct1) and Vt or Mvt (0.6 molar ratio amount)(Ct2) were cosedimented separately. A) Each of Vt, Mvt, Mvt R975W, and Mvt L954del were sedimented with F-actin. B) Cosedimentation was conducted using equimolar mixtures of Vt and Mvt (wild-type and mutant).

appeared in the supernatant. In each case, Vt along with wild-type and mutant Mvt produced similar results (n = 2). The intensities of Vt and Mvt bands on the gels were generally faint at the 0.3 molar ratio, and the degree of staining intensified with increasing ratios. Although the gels visually appear similar, densitometric analysis of (meta)vinculin bands was somewhat variable (Table 3.1). At higher molar ratios, a greater proportion of total (meta)vinculin tail appeared to pellet with the actin than at the 0.3 molar ratio

(generally 45% versus 25%). This observation may be attributed to a cooperative effect at increased ratios, since greater amounts of (meta)vinculin may result in increased dimerization and therefore increased cosedimentation with F-actin. Furthermore, reduced amounts of protein at the 0.3 ratio and subsequent weak staining of bands on the gels may have contributed to this result.

Table 3.1 Percentages of total (meta)vinculin tail pelleting with F-actin in two separate cosedimentations as determined by densitometric analysis of SDS-PAGE.

Protein	0.3 molar ratio	0.6 molar ratio	0.9 molar ratio
Vt	21.8, 25.3	38.0, 41.2	35.5, 67.1
Mvt	26.6, 34.6	42.2, 43.9	40.2, 44.3
Mvt R975W	23.7, 26.6	23.4, 43.2	36.5, 48.9
Mvt L954del	37.3, 38.3	33.8, 38.1	37.2, 50.5

Since interactions with F-actin promote homodimerization of vinculin (Janssen, et al. 2006), the possibility that the heterodimerization of vinculin and metavinculin might also be enhanced and affect actin binding was considered. F-actin cosedimentation assays were repeated with equimolar amounts of Vt and Mvt (Fig 3.10B). SDS-PAGE and densitometric analysis revealed similar binding of the proteins to F-actin as when they were cosedimented separately. Thus, if heterodimerization occurred it did not affect actin binding.

In addition to binding F-actin, vinculin and metavinculin have the ability to cross-link actin filaments through their homo- (and presumably hetero-) dimerization upon F-actin binding (Janssen, et al. 2006; Olson, et al. 2002). The cross-linking of F-actin by Vt and wild-type and mutant Mvt was evaluated using falling ball viscometry. In this

method, a stainless steel ball was dropped through a capillary tube containing polymerized actin and its rate of descent recorded. The viscosity of the actin solution was then calculated using a standard calibration curve. In the absence of (meta)vinculin an average viscosity of 10.4 cP (n = 3) was mesured. Viscosities much greater than this value indicate the formation of a cross-linked actin meshwork, while viscosities lower than this value suggest actin bundling. F-actin polymerized separately with Vt or Mvt generally resulted in viscosities similar to that of the actin alone at all three molar ratios (Fig. 3.11A), except at the 0.3 molar ratio, where Vt yielded a relatively high average viscosity of 287 cP, compared to those of wild-type or mutant Mvt. There did not appear to be much difference in viscosity among wild-type or mutant Mvt at any of the three ratios. Thus homodimerization of Vt promotes network formation more effectively at a low molar ratio, but otherwise all four proteins behave in a similar manner regarding the cross-linking of F-actin.

Interestingly, F-actin that was polymerized with an equimolar mixture of Vt and Mvt resulted in considerably higher viscosities (Fig. 3.11B), indicating that filamentous F-actin networks were more readily formed in the presence of Vt-Mvt heterodimers. Combinations of Vt-Mvt and Vt-Mvt L954del yielded similar trends, with viscosities peaking at approximately 1000 cP at the 0.6 molar ratio. The Vt-Mvt R975W mixture

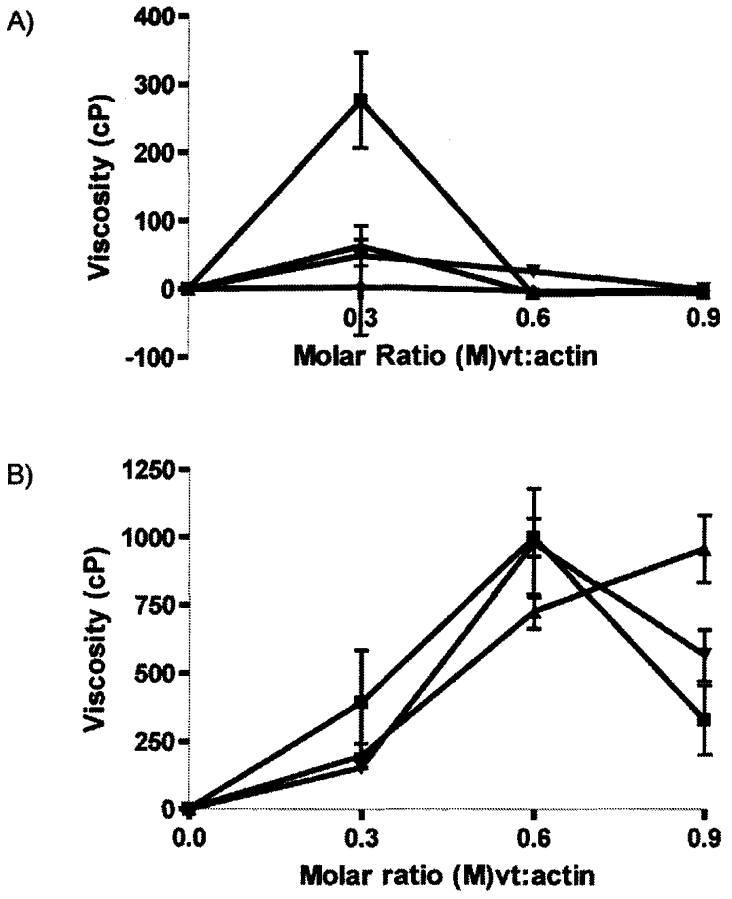

Fig. 3.11 Viscosities of solutions of polymerized F-actin incubated with Vt (■), Mvt (▲), Mvt R975W (▼), or Mvt L954del (◆) in 0.3, 0.6, and 0.9 molar ratios (meta)vinculin:actin. The viscosity of polymerized F-actin in the absence of (meta)vinculin (10.4 cP) was substracted from each value. F-actin was allowed to polymerize in the presence of Vt or Mvt A) separately and B) in equamolar mixtures of Vt-Mvt (■), Vt-Mvt R975W (▲), or Vt-Mvt L954del (▼).

also showed high viscosities, though it revealed a maximum viscosity at the 0.9 ratio. To examine the effects of the Vt-Mvt ratio, the assay was repeated with a 20, 40, 50, 60, and 80% Mvt molar amount of total (meta)vinculin at a 0.6 ratio to actin. Viscosities were generally found to peak in the presence of 50-60% Mvt (of total (meta)vinculin), indicating that approximate equimolar amounts of Vt and Mvt are most effective at

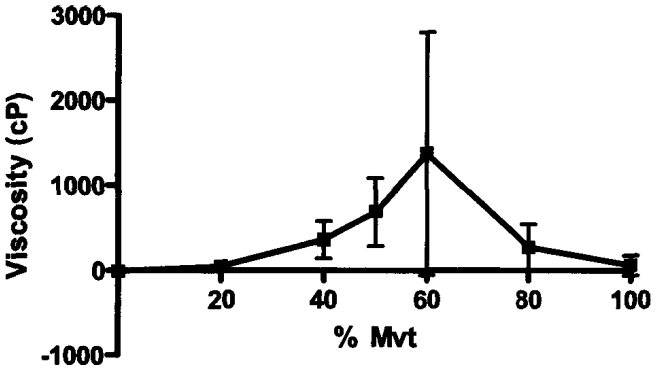

Fig. 3.12 Viscosities of solutions of polymerized F-actin incubated with increasing percentages of Mvt (of total (meta)vinculin) at a 0.6 molar ratio (meta)vinculin:actin.

forming networks of actin filaments (Fig. 3.12). At this ratio, equimolar amounts of Vt and Mvt incubated with F-actin yielded significantly higher viscosities ($n = 12$) ($P < 0.05$) than Vt or Mvt separately (~1000 cP vesus ~10 cP).

To extend the above observation and look at a possible requirement for conformational change, certain disulfide-bonded mutants of Vt were tested in the falling-ball assay in mixtures with Mvt at the (meta)vinculin:actin 0.6 molar ratio. The Vt straplock (P878C, S913C), armlock (S913C, Q1066C), and terminal-lock (P878C, Q1066C) proteins were purified and oxidized by Courtney Voss of the Ball lab, and in their oxidized forms have restricted motion of the N-terminal strap (residues 878-896) and/or the C-terminal arm (residues 1048-1066) of the Vt protein (Fig. 3.13). Trials were conducted ($n = 3$) using these disulfide mutant Vt proteins in their oxidized and reduced forms in both equimolar amounts to Mvt and in amounts increased threefold to compensate for their reduced actin binding. Oxidized forms of the Vt straplock and Vt

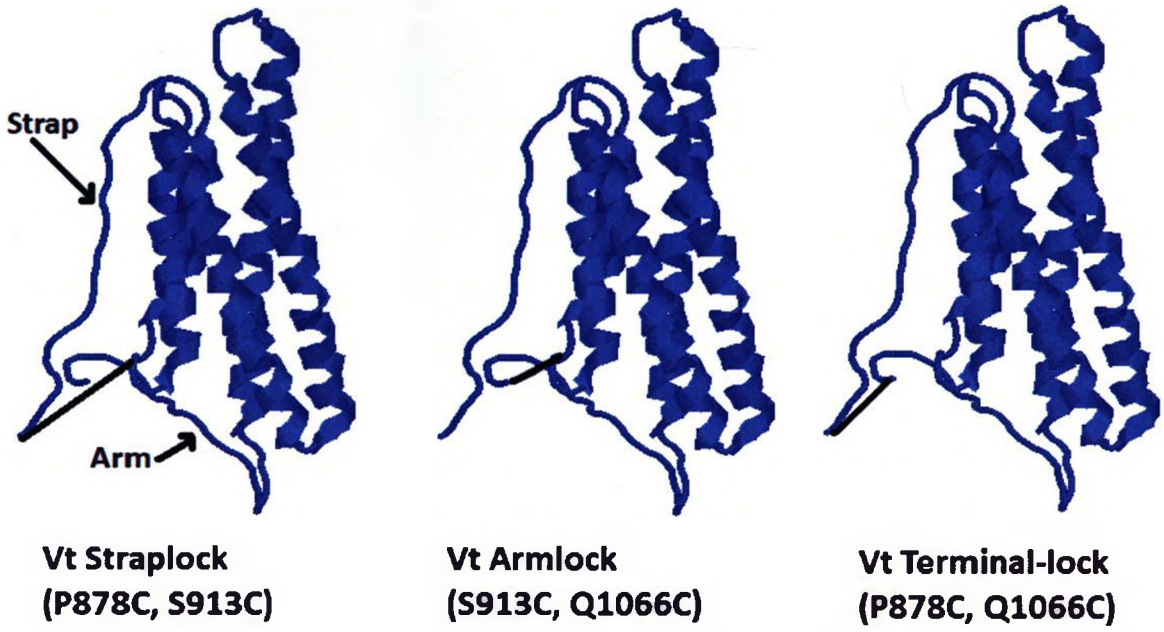

Fig. 3.13 Cartoon representations of the Vt straplock, armlock and terminal-lock proteins, adapted from Bakolitsa *et al.* (Bakolitsa, et al. 2004)(PDB ID: 1ST6). The locations of the strap and arm portions of Vt are indicated with arrows, and the disulfide bonds occurring in oxidized forms of the proteins are indicated with black lines.

armlock produced similar results to that of unmutated Vt, producing actin solutions of relatively high average viscosity (1375 +/- 306 cP and 433 +/- 96 cP, respectively), thus providing evidence of filamentous network formation. The oxidized Vt terminal-lock protein, which fixes both the strap and arm in place, resulted in greatly reduced average viscosity in both Mvt-equimolar and triplicate amounts (17 cP and 36 cP, respectively), indicating much less actin network formation. When the Vt terminal-lock protein was reduced and incubated in an amount equimolar to Mvt, network formation was evident with an average viscosity of 428 +/- 25 cP, thus providing evidence that movement of both the Vt strap and arm is required for dimerization.

Another-actin binding protein that binds vinculin and has the potential to be involved in heart function is VASP (Brindle, et al. 1996). Interactions between Mvt and

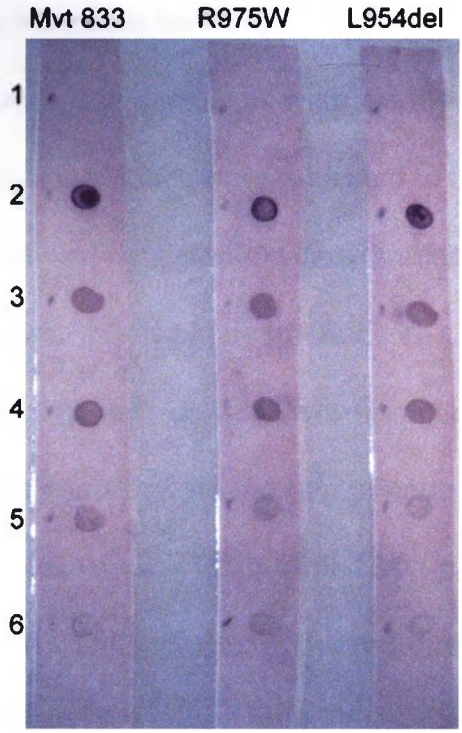

Fig. 3.14 Binding of GST-EVH1 to Mvt. Strips of nitrocellulose with bound Mvt are shown after binding and development. Spotting order for each strip is as follows: 1) 1 µg BSA, 2) 0.02 µg GST, 3)-6) Mvt 833 (wild-type or mutant) in amounts of 1 µg, 0.5 µg, 0.1 µg, and 0.05 µg, respectively.

the EVH1 domain of the VASP protein were examined using a simple nitrocellulose overlay assay to determine if the metavinculin mutations affect this interaction. The assays were conducted using Mvt 833 constructs (vinculin hinge + metavinculin tail, residues 833-1134) which include a known EVH1 binding site at residues 839-843 within the vinculin hinge region. Wild-type and mutant Mvt 833 were spotted onto separate strips of nitrocellulose, probed with a GST fusion of EVH1, and protein interactions detected. On each strip, the degree of staining decreased correspondingly as the amount of spotted Mvt 833 was reduced, and staining at Mvt 833 (spot #3-6) was less intense than at the GST positive control (spot #2). There were no apparent differences in EVH1 interactions among wild-type and mutant metavinculin (n = 2)(Fig. 3.14) as is shown by similar degrees of stain intensity at their respective spots.

Since no differences were seen between mutant and wild-type metavinculin in interactions with known ligands, some attempts were made to identify novel ligands. First, extracts from a variety of rat tissues were subjected to SDS-PAGE and blotted to a nitrocellulose membrane, followed by guanidine denaturation and subsequent renaturation. The membrane was subsequently probed with GST-Mvt to look for binding proteins, however, no interactions were detected (results not shown).

Binding of fluorescently labelled Vt and Mvt to permeabilized cells was also analyzed. The NCys (P878C) mutations within Vt and Mvt proteins were labelled with fluorescein-5-maleimide (F5M). F5M-labelled NCys proteins were prepared to final concentrations of between 0.3 and 0.9 mg/mL with F5M:protein ratios of approximately 0.7. F5M-labelled Mvt proteins were subjected to SDS-PAGE and the gel viewed and photographed under UV light to examine labelling of the proteins (Fig. 3.15).

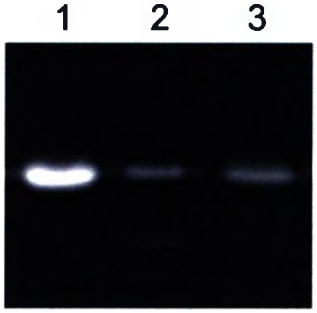

Fig. 3.15 Labelling of NCys-Mvt L954del (lane 1), NCys-Mvt R975W (lane 2), and NCys-Mvt (lane 3) with fluorescein-5-maleimide. Labelled proteins were subjected to SDS-PAGE and viewed under UV light.

Cultured U2OS cells (human bone osteosarcoma) were permeabilized with triton X-100 and incubated with fluorescein-labelled NCys-Vt or -Mvt, and with rhodamine-labelled phallacidin to analyze F-actin. Cell clusters were viewed with a microscope equipped with appropriate fluorescent filters and photographed. The rhodamine-phallacidin bound actin filaments throughout the cells as was evident by the clearly

visible red-colored actin cytoskeleton (Fig 3.16A). Such staining was observed both at cellular boundaries, and at stress fibers throughout the cells. The staining patterns of Vt and Mvt were identical in appearance, and were identical to that of phallacidin (with the exception of apparent nuclear staining). Resulting photographs were artificially colored red or green (Fig. 3.16A) and images were overlaid, yielding an orange or yellow color in locations where both F5M-Vt/Mvt and rhodamine-phallacidin were present (Fig. 3.16B). The overlaid images give the cells an orange-yellow appearance throughout, since Vt/Mvt and phallacidin bound the cells in the same locations. Cells incubated with Vt, Mvt, R975W, and L954del did not appear to exhibit any differences in appearance or staining patterns.

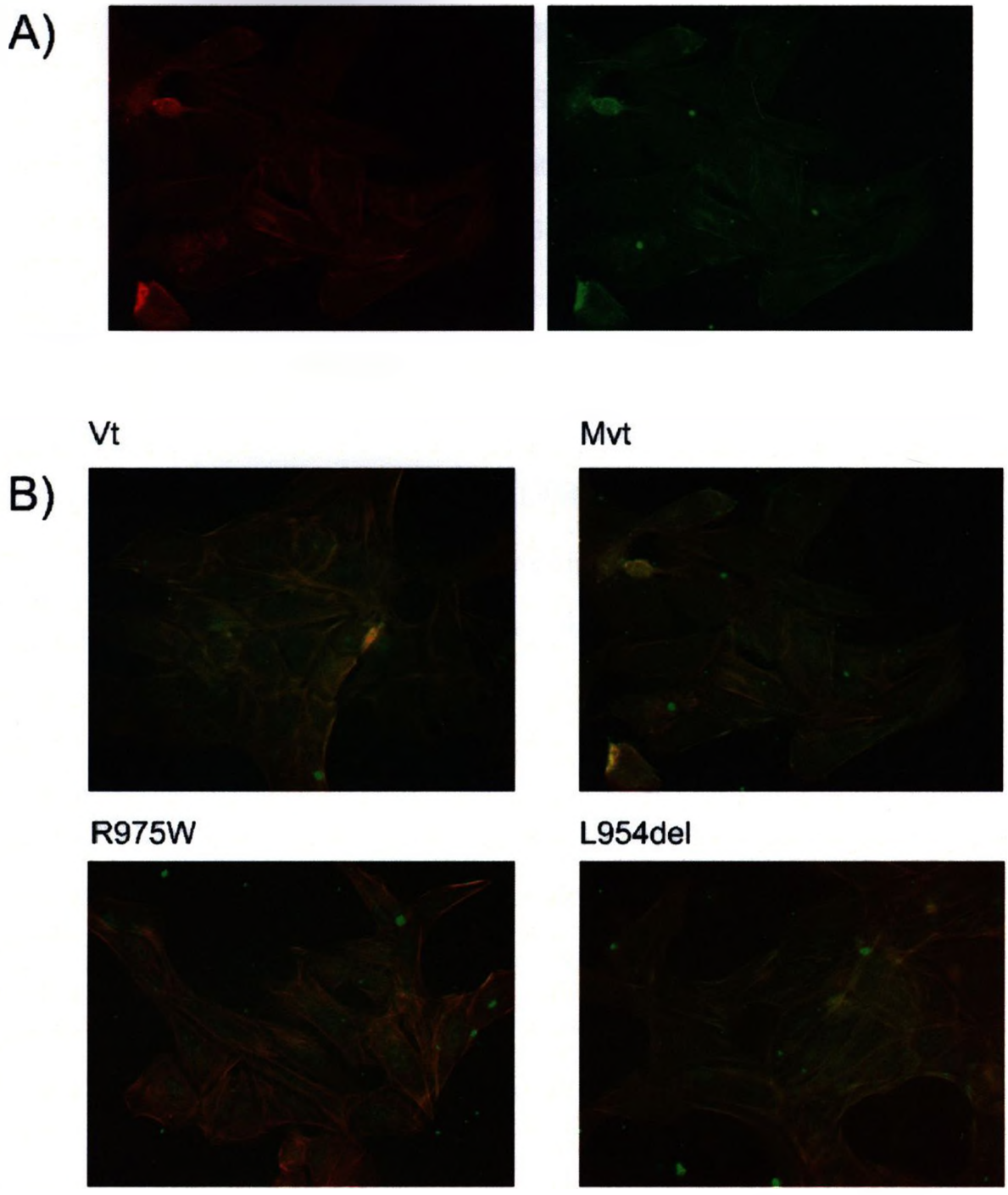

Fig. 3.16 A) Photographs of cells labelled with rhodamine-phallacidin (left) and NCys-Mvt (right). B) Overlaid colored photographs of permeabilized U2OS cells incubated with rhodamine-phallacidin and F5M-labelled NCys-Vt, NCys-Mvt, NCys-Mvt R975W, and NCys-Mvt L954del.

CHAPTER 4

DISCUSSION

The intent of this study was to investigate structural differences between wild-type metavinculin tail (Mvt) and its R975W and L954del mutants and to examine differences in interactions among these Mvt variants and certain known ligands in order to gain insight into the function of metavinculin. In most cases, the properties of wild-type and mutant Mvt were found to be identical. The R975W mutant exhibits slightly reduced thermal stability relative to the wild-type and L954del proteins, and wild-type Mvt may have a greater degree of exposed hydrophobic surface than the two mutants. A novel finding was a synergistic effect of Vt and Mvt in the formation of filamentous actin networks.

4.1 Physical Properties of Wild-Type and Mutant Metavinculin

Although the structures of human and chicken Vt have been determined (Bakolitsa, et al. 1999; Bakolitsa, et al. 2004; Borgon, et al. 2004), little is known regarding the structure of the 68 amino-acid metavinculin insert or how it may change the Vt structure. Since the deletion of the insert (Maeda, et al. 1997), and R975W and L954del mutations within the insert (Olson, et al. 2002) have been associated with DCM, it is evident that the insert provides metavinculin with some unique function relative to vinculin. This study evaluated several physical properties of Mvt, and the results provide insight both into the structure of the metavinculin insert, and the effects of the R975W and L954del mutations on the structure and stability of the Mvt protein.

The insert sequence was previously analyzed (Olson, et al. 2002) using the Garnier-Robson algorithm (Levin, Robson and Garnier 1986) and was predicted to form

three helices (M1, M2, and M3) (Fig. 1A), the first two of which are acidic and the third being basic. However, in the absence of a homologous protein of known structure (as is the Mvt insert), the algorithm is only 60-65% accurate (Garnier, et al. 1990; Levin, Robson and Garnier 1986), and certain discrepancies are noted regarding the predicted

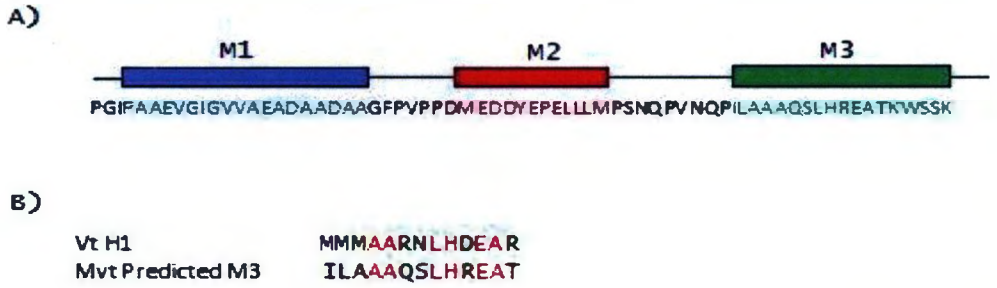

Fig. 4.1 A) Predicted structure of the metavinculin insert as described by Olson *et al.* displaying the M1, M2, and M3 helical regions (Olson, et al. 2002). B) Alignment of the H1 helix of Vt and the predicted M3 helix of Mvt. Aligned residues are colored in red.

structure and known sequence. The M1 helix contains a glycine-isoleucine-glycine motif and the M2 helix a single proline, both of which are in central locations of the predicted helices. The unique structures of glycine and proline result in their low degrees of helical propensity (Chou and Fasman 1978), and indeed these residues are often found to terminate helices. As the N-terminal portion of the insert is taxonomically variable both in length and sequence (Strasser, et al. 1993), it may form a series of smaller helices or be relatively disordered. Indeed, the protein disorder prediction tools PONDR VL-XT (Li, et al. 1999; Romero, Obradovic and Dunker 1997; Romero, et al. 2001)(Molecular Kinetics Inc., Indianapolis, IN) and DisEMBL (Linding, et al. 2003) estimated a large portion of this region (residues 910-950) to be disordered. However, the prediction of a helical structure in the M2 region might be accurate, with the proline at position 951 kinking the

helix in a similar manner as the P989 residue within helix 4 (H4) of the Vt (Bakolitsa, et al. 1999). It is interesting to note that there are similarities within the sequences of helix 1 (H1) of Vt and the predicted M3 of the metavinculin insert (Fig. 1B), and since the H1 and H2 helices are arranged in an antiparallel manner within Vt (Bakolitsa, et al. 1999), it is possible that M3 displaces H1 within the Mvt structure.

The R975W and L954del mutations within the metavinculin insert have been associated with the onset of dilated cardiomyopathy (Olson, et al. 2002). Although the structure of the metavinculin insert is not known, a multiple sequence alignment of metavinculin proteins from several species indicate that both R975 and L954 occur in the highly conserved C-terminal half of the insert (see Fig. 1.3). Furthermore, L954 was conserved among all species in the alignment, and R975 among all species with the exception of the zebrafish, where it was substituted with a glutamine. The R975 residue is located near the C-terminal of the insert within the predicted M3 helix, and L954 the second of three consecutive leucine residues within the predicted M2. If indeed the M3 helix of the insert displaces H1 of Vt and packs together with H2, the polar R975 is likely to be exposed to the solvent and may be of importance in ionic interactions between the two helices. The L954 residue may also be of importance within its leucine triplet, as it may be involved in contacts with an ILAAA segment at the beginning of M3, since these are two stretches of aliphatic amino acids in close proximity. In some support of these predictions, studies conducted by Andrew Swindell and Aakash Shah of the Ball lab using cysteine mutations at these positions have provided evidence that both positions are exposed to the solvent (personal communication).

The mutation of the highly basic arginine residue at position 975 to a large and hydrophobic tryptophan residue might be expected to alter the conformation of the protein such that the tryptophan residue is partially or fully occluded from the solvent (Cordes and Sauer 1999; Schwehm, et al. 1998). Furthermore, one might speculate that inter-helical interactions could be affected by the R975W mutation, since R975 may have a role in maintaining polar interactions among residues in adjacent helices. If the M2 region indeed forms a helix, the deletion of L954 will presumably shorten the helix and might interfere with hydrophobic packing between the predicted M2 and M3 helical regions and thus distort the molecule. Thus, to examine the effects of these mutations on the structure and stability of metavinculin, the thermal stability, resistance to proteolysis, and exposed hydrophobic surface of wild-type and mutant Mvt were evaluated and compared.

The observation of increased heat sensitivity may indicate that the R975W mutation results in a local reorganization of the molecule to bury the tryptophan residue though no indication of conformational change relative to the wild-type was observed by proteolysis. The R975W mutation may also result in a "reverse hydrophobic effect" (Pakula and Sauer 1990) in which the stability of the denatured form of the protein is increased, thus leading to reduced thermal stability at high temperatures. On the other hand melting temperature of the L954del mutant did not differ significantly from that of the wild-type, which suggests that this mutation does not greatly alter the conformation or stability of the protein. Furthermore, although the T_m of Mvt R975W was found to be significantly lower than that of wild-type Mvt, it is still about 30°C greater than the

normal body temperature of 37°C. Therefore, all three proteins should be highly stable under physiological conditions.

Limited proteolysis results not only point to identical conformations of wild-type and mutant Mvt, but also suggest that a portion of the metavinculin insert is very sensitive to proteolysis and thus is likely extended from the protein. Courtney Voss of the Ball Lab has previously found that the vinculin tail (Vt) protein is highly resistant to degradation by protease K (personal communication). Since a 22 kDa fragment results from the degradation of wild-type and mutant Mvt (Fig. 3.2), this supports the theory that the predicted M3 region of the metavinculin insert displaces H1 of Vt to form a Vt-like helical bundle, which like Vt is resistant to protease K proteolysis. Furthermore, since Mvt is more readily degraded by protease K than Vt, this may provide further evidence of structural disorder within the N-terminal portion of the metavinculin insert. However, a sensitive method of analysis such as mass spectrometry would be required to further examine the composition of the residual fragment.

Since protease K degradation of the proteins provides some evidence of structural similarity, it was thought that the mutants might reveal similar degrees of exposed hydrophobic surface as the wild-type. The more intense emission spectrum of wild-type Mvt than the two mutants in an excess of ANS suggests that wild-type Mvt is slightly more hydrophobic than its two mutants, the reverse of what might be expected. However, all three proteins showed similar affinities for phenylsepharose, indicating similar degrees of hydrophobicity. The increased fluorescent signal that was observed from ANS in the presence of wild-type Mvt relative to the mutants may have occurred as a result of either discrepancies in protein concentration estimation or the presence of protein contaminants

or degradation products within the Mvt sample that was used, though neither explanation seems likely. It is also important to note that all three proteins yielded spectra that were only slightly greater than that of ANS in the absence of protein. Relative to calmodulin, the fluorescence enhancement was small (15 000 cps vs. 45 000 cps). Therefore, even if wild-type Mvt does exhibit increased hydrophobicity relative to the mutants, the difference is marginal as all three spectra reveal the proteins to display largely hydrophilic surfaces.

4.2 Biological Properties and Interactions of Metavinculin

Since little evidence of conformational differences was found among wild-type and mutant Mvt, the possibility that binding interactions were altered by the mutations was investigated.

The intramolecular interaction that is thought to regulate metavinculin was examined using an assay in which Mvt competed with fluorescently-labelled Vt-K944C for Vh, and no differences were observed among wild-type and mutant Mvt. The known Vh binding sites within Mvt are C-terminal to the site of the insert (Bakolitsa, et al. 2004) and thus any conformational changes that the R975W and L954del may inflict on the Mvt protein likely do not negatively impact the Mvt-Vh interaction. These results are further supported by gel filtration analysis of Vh and Mvt that was conducted by Lauren McCullagh of the Ball lab, which also did not indicate any differences in Vh interactions among wild-type and mutant Mvt (unpublished results).

The fluorescent competitive binding assay used here revealed the affinities of wild-type and mutant Mvt for Vh to be similar to values previously reported for the Vt-Vh interaction (50-100 nM) (Johnson and Craig 1994; Miller, Dunn and Ball 2001; Witt,

et al. 2004). In contrast to these results, the binding of Mvt to Vh has previously been characterized using surface plasmon resonance (Witt, et al. 2004), giving an affinity of Mvt for Vh (Kd = 336 nM); significantly reduced relative to Vt (Kd = 50 nM). The reason for these differing results is not clear. However, Witt *et al.* used larger Vt and Mvt constructs which included a portion of the hinge region (residues 858-1066 and 858-1134, respectively)(Witt, et al. 2004), and the presence of these extra residues in conjunction with the insert may have possibly influenced the Mvt-Vh interaction.

Binding sites for lipid in Vt have been identified as including a "basic ladder" in H3, and a basic collar by mutational analysis (Chandrasekar, et al. 2005; Johnson, et al. 1998). Interestingly, this vinculin-lipid interaction is predicted to have a role in focal adhesion turnover (Chandrasekar, et al. 2005; Saunders, et al. 2006). Metavinculin was previously found to have reduced affinity for acidic phospholipids relative to vinculin, possibly because of the acidic nature of the metavinculin insert (Witt, et al. 2004), and the results of the PIP strip overlay and lipid cosdeimentation assays supports this finding. A surprising result was the apparent specificity among both Vt and Mvt for PtdIns(3)P and PtdIns(5)P. The interactions of vinculin and metavinculin with variants of PI-monophosphates have not been well characterized, though a previous study indicated that PI-bisphosphates and PtdIns(3,4,5)P3 more readily activated autoinhibited vinculin than PtdIns(3)P and PtdIns(4)P (Steimle, et al. 1999). Although protein-lipid overlay assays can be an inexpensive and simple means of detecting protein-lipid interactions (Dowler, Kular and Alessi 2002) the manufacturer of PIP strips (Echelon Biosciences) cautions that such analyses may produce different binding patterns compared to other assays and that protein-lipid specificity can vary with different protein concentrations and buffer

conditions. The manufacturer further recommends that alternate experiments be conducted to further characterize protein-lipid interactions, and another study acknowledges that although protein-lipid overlay assays may be sensitive, their results must be interpreted with caution (Yu, et al. 2004). Thus, more weight should be given to the results of the lipid cosedimentation assays. These results confirmed that Vt has greater affinity for acidic phospholipids than Mvt (Witt, et al. 2004), and did not detect any differences in affinity for the phospholipids among wild-type and mutant Mvt. Thus it is likely that wild-type and mutant Mvt are cycled at cellular junctions to a similar degree.

The binding of acidic phospholipids (Witt, et al. 2004) and F-actin (Janssen, et al. 2006; Johnson and Craig 2000) are believed to expose cryptic dimerization sites within Vt and Mvt, as detected by chemical cross-linking. Some evidence of preferential heterodimerization of lipid-incubated vinculin with metavinculin has been reported (Witt, et al. 2004). In contrast to these results, I found that Mvt and Vt incubated with PI revealed similar degrees of heterodimerization in a nitrocellulose overlay assay; these differing observations may have occurred either because different phospholipids (PI versus PIP_2) or different (meta)vinculin tail constructs (from residue 858 versus 877) were used in the analysis. The overlay assay and gel filtration analysis also confirmed that dimerization will not occur in the absence of lipid, providing evidence that the lipid induces and/or stabilizes a conformational change in the proteins to expose sites of dimerization.

The homo- and heterodimerization properties of wild-type and mutant Mvt were not found to differ. Metavinculin is presumed to be involved in the organization of actin through its dimerization and subsequent cross-linking of actin filaments, and the similar

results of the falling ball viscometry assay with wild-type and mutant Mvt provide further evidence that all three proteins have similar dimerization properties. It has been predicted that movement of the N-terminal strap (residues 878-896) and C-terminal arm (residues 1048-1066) are required in order to expose dimerization sites. The R975W and L954del mutations are likely not in close proximity to these regions and the mutants do not differ from the wild-type in their affinities for dimer-inducing acidic phospholipids or F-actin. Thus, these mutations do not alter the dimerization properties of metavinculin.

Since a major part of vinculin (and by comparison metavinculin) function is thought to be in the binding of actin, it was of interest to look for differences in the interactions of wild-type and mutant Mvt with F-actin. Electron microscopy and modeling studies have predicted Vt to bind to two G-actin monomers within an F-actin filament at two distinct sites; one at the top and one at the base of H3 (Janssen, et al. 2006). Actin cosedimentation assays found wild-type and mutant Mvt to have similar affinities for F-actin, and is in agreement with a previous study (Olson, et al. 2002). F-actin and acidic phospholipids bind vinculin at overlapping sites, and their binding to Vt has been shown to be mutually exclusive (Steimle, et al. 1999). Since the actin binding sites are downstream from the insert and since the mutations do not affect lipid interactions, it is perhaps not surprising that F-actin affinities are also unaltered.

In addition to simply binding F-actin, vinculin and metavinculin are involved in the cross-linking and therefore organization of actin filaments. Actin structures inside the cell range from parallel-stacked bundles to three-dimensional networks in which filaments are arranged in a web-like array (Korneeva and Jockusch 1996). Past studies reported that vinculin promotes actin bundling while metavinculin induces network

formation- an interesting difference between the two proteins (Olson, et al. 2002; Rudiger, et al. 1998). Olson *et al.* examined actin organization by the R975W and L954del mutant forms of metavinculin using a low-shear viscometry assay with a falling-ball apparatus and reported that the mutants behaved in a manner similar to vinculin rather than metavinculin. It was suggested that the altered actin organizing ability displayed by the mutants might affect the intercalated discs of cardiac muscle and the subsequent onset of dilated cardiomyopathy. I wished to re-examine the mutants in this assay particularly with regard to the possibility of heterodimerization. My results showed that Vt greatly increased viscosity (and thus promoted network formation) relative to Mvt at the 0.3 molar ratio, contrary to the previously published result (Olson, et al. 2002). Olson *et al.* also provided evidence that wild-type Mvt yielded viscosities 20-50 fold higher than the actin control, peaking at the 0.6 molar ratio. In contrast to that observation, I found that wild-type Mvt behaved in a similar manner to the two mutants, with viscosities similar to that of the actin control at all three ratios. The reason for these differing results is unclear, though Olson *et al.* used larger Vt and Mvt constructs (residues 858-1066 and 858-1134, respectively)(Olson, et al. 2002)(Witt, et al. 2004), and the presence of these additional residues in conjunction with the insert may have possibly influenced the (meta)vinculin-actin interaction. Furthermore, my study used a higher concentration of F-actin as compared to the assay of Olson *et al.*, (0.3 mg/mL versus 0.13 mg/mL), and this discrepancy may also have led to these different results.

When the assay was conducted with equimolar mixtures of Vt and Mvt, viscosities increased by a factor of several-hundred fold as compared to separate incubations with Vt or Mvt. As was observed with separate Mvt in a published study

(Olson, et al. 2002), viscosity of the equimolar Vt-Mvt mixtures peaked at the 0.6 molar ratio. This effect was lost when a "locked" Vt mutant was used, in which the N-terminal strap and C-terminal arm are covalently linked, which provides further support to the theory of Janssen et al that movement of the N- and C-terminal regions of Vt is necessary for dimerization sites to be exposed (Janssen, et al. 2006). Similar viscometric trends were observed among Vt-Mvt, Vt-Mvt R975W, and Vt-Mvt L954del ratios, indicating that the mutations likely do not alter actin organizational properties of Mvt. It is important to note that particularly in solutions of high viscosity, this method yields viscometric measurements of high variability (MacLean-Fletcher and Pollard 1980; Pollard and Cooper 1982). The assay was repeated at the 0.6 molar ratio with mixtures containing increasing molar percentages of wild-type Mvt (of total (meta)vinculin) to examine the effect of the Vt-Mvt ratio. Although there was a general trend of maximal viscosity at 50-60% Mvt, measured viscosities were highly variable. Furthermore, rates of actin gelation were found to be variable, as varied incubation periods of polymerization yielded inconsistent results (not shown). Therefore, because of the variability of measured viscosities, small differences in actin organization among wild-type and mutant metavinculin might exist. The high viscosity obtained with equal amounts of Vt and Mvt suggest that the heterodimerization of Vt and Mvt is most favourable for the subsequent formation of actin networks. Although the structure of the metavinculin insert is not known, it is conceivable that the insert orients the actin-bound Mvt protein in such a way that network formation is favoured upon heterodimerization with a neighboring actin-bound Vt protein. As a further analysis it would be interesting to conduct electron microscopic analysis and subsequent computer modelling as described by Janssen *et al.*

(Janssen, et al. 2006) of actin polymerized with Vt and Mvt to further examine this phenomenon.

To examine interactions of Mvt in a more natural context, cultured cells were permeabilized and incubated with fluorescein-labelled NCys variants of the Mvt and Vt proteins. Photographic analysis revealed all four proteins to localize to cellular actin filaments, giving an identical pattern to phallacidin. At this level of resolution, cells incubated with wild-type and mutant metavinculin were similar in appearance, providing further evidence that the mutations do not alter the metavinculin-actin interaction.

VASP is known to have a role in actin filament formation (Krause, et al. 2003), and has been implicated in the onset of DCM (Eigenthaler, et al. 2003). The mutations were expressed in the extended Mvt 833 construct which includes a known binding site for the EVH1 domain of the VASP protein (Brindle, et al. 1996), and overlay assays indicated that wild-type and mutant Mvt 833 do not differ in their affinities for the EVH1 domain of VASP. A second putative VASP binding site was identified within the metavinculin insert (residues 939-943), and Sarah Aubut of the Ball lab detected an EVH1 interaction at this site when position 939 was modified (unpublished data). Thus, mutations in the metavinculin insert might alter VASP interactions at this location. However, the mutants appeared normal in this respect, with no interactions detected with GST-EVH1 among any of the proteins.

In conclusion, these experiments examined the structure and interactions of wild-type and mutant metavinculin to help explain the role of the R975W and L954del mutations in dilated cardiomyopathy. With the exception of some small structural

differences, the surveyed binding properties of wild-type and mutant Mvt appear to be identical.

4.4 Future Directions

To further investigate the role of these mutations, the interactions of Mvt with other known ligands could be evaluated. In addition to the ligands that were studied, (meta)vinculin is known to bind paxillin (Wood, et al. 1994), raver1 (Huttelmaier, et al. 2001), α-synemin (Sun, et al. 2008), and protein kinase C (Weekes, Barry and Critchley 1996), and it is possible that the R975W and L954del mutations affect the binding properties of Mvt to any or all of these proteins. It is also possible that these metavinculin mutations alter interactions with one or more unknown ligands that remain to be discovered. Furthermore, it would be important to observe the mutations within the context of the full-length metavinculin protein. Under these circumstances it is possible that the mutations somehow affect the conformation of the head and/or hinge regions of the protein and may influence interactions with their respective ligands. Furthermore, solving the metavinculin insert structure will provide an increased understanding of its conformation and role within the metavinculin insert, and will help to predict possible distortions and subsequent altered ligand interactions that may result from the R975W and L954del mutations, leading to the onset of dilated cardiomyopathy.

REFERENCES

Alatortsev, V. E., Kramerova, I. A., Frolov, M. V., Lavrov, S. A. and Westphal, E. D. (1997) Vinculin gene is non-essential in Drosophila melanogaster. *FEBS Lett.* **413,** 197-201.

Bakolitsa, C., Cohen, D. M., Bankston, L. A., Bobkov, A. A., Cadwell, G. W., Jennings, L., Critchley, D. R., Craig, S. W. and Liddington, R. C. (2004) Structural basis for vinculin activation at sites of cell adhesion. *Nature* **430,** 583-586.

Bakolitsa, C., de Pereda, J. M., Bagshaw, C. R., Critchley, D. R. and Liddington, R. C. (1999) Crystal structure of the vinculin tail suggests a pathway for activation. *Cell* **99,** 603-613.

Ball, E. H. (1986) Quantitation of proteins by elution of Coomassie brilliant blue R from stained bands after sodium dodecyl sulfate-polyacrylamide gel electrophoresis. *Anal. Biochem.* **155,** 23-27.

Ball, E. H., Freitag, C. and Gurofsky, S. (1986) Vinculin interaction with permeabilized cells: disruption and reconstitution of a binding site. *J. Cell Biol.* **103,** 641-648.

Barstead, R. J. and Waterston, R. H. (1991) Vinculin is essential for muscle function in the nematode. *J. Cell Biol.* **114,** 715-724.

Bass, M. D., Patel, B., Barsukov, I. G., Fillingham, I. J., Mason, R., Smith, B. J., Bagshaw, C. R. and Critchley, D. R. (2002) Further characterization of the interaction between the cytoskeletal proteins talin and vinculin. *Biochem. J.* **362,** 761-768.

Belkin, A. M., Ornatsky, O. I., Glukhova, M. A. and Koteliansky, V. E. (1988) Immunolocalization of meta-vinculin in human smooth and cardiac muscles. *J. Cell Biol.* **107,** 545-553.

Bois, P. R., O'Hara, B. P., Nietlispach, D., Kirkpatrick, J. and Izard, T. (2006) The vinculin binding sites of talin and alpha-actinin are sufficient to activate vinculin. *J. Biol. Chem.* **281,** 7228-7236.

Borgon, R. A., Vonrhein, C., Bricogne, G., Bois, P. R. and Izard, T. (2004) Crystal structure of human vinculin. *Structure* **12,** 1189-1197.

Bowles, K. R., Gajarski, R., Porter, P., Goytia, V., Bachinski, L., Roberts, R., Pignatelli, R. and Towbin, J. A. (1996) Gene mapping of familial autosomal dominant dilated cardiomyopathy to chromosome 10q21-23. *J. Clin. Invest.* **98,** 1355-1360.

Brindle, N. P., Holt, M. R., Davies, J. E., Price, C. J. and Critchley, D. R. (1996) The focal-adhesion vasodilator-stimulated phosphoprotein (VASP) binds to the proline-rich domain in vinculin. *Biochem. J.* **318 (Pt 3),** 753-757.

Chandrasekar, I., Stradal, T. E., Holt, M. R., Entschladen, F., Jockusch, B. M. and Ziegler, W. H. (2005) Vinculin acts as a sensor in lipid regulation of adhesion-site turnover. *J. Cell. Sci.* **118,** 1461-1472.

Chou, P. Y. and Fasman, G. D. (1978) Prediction of the secondary structure of proteins from their amino acid sequence. *Adv. Enzymol. Relat. Areas Mol. Biol.* **47,** 45-148.

Coll, J. L., Ben-Ze'ev, A., Ezzell, R. M., Rodriguez Fernandez, J. L., Baribault, H., Oshima, R. G. and Adamson, E. D. (1995) Targeted disruption of vinculin genes in F9 and embryonic stem cells changes cell morphology, adhesion, and locomotion. *Proc. Natl. Acad. Sci. U. S. A.* **92,** 9161-9165.

Cordes, M. H. and Sauer, R. T. (1999) Tolerance of a protein to multiple polar-to-hydrophobic surface substitutions. *Protein Sci.* **8,** 318-325.

DeMali, K. A., Barlow, C. A. and Burridge, K. (2002) Recruitment of the Arp2/3 complex to vinculin: coupling membrane protrusion to matrix adhesion. *J. Cell Biol.* **159,** 881-891.

Dowler, S., Kular, G. and Alessi, D. R. (2002) Protein lipid overlay assay. *Sci. STKE* **2002,** PL6.

Ebeling, W., Hennrich, N., Klockow, M., Metz, H., Orth, H. D. and Lang, H. (1974) Proteinase K from Tritirachium album Limber. *Eur. J. Biochem.* **47,** 91-97.

Eigenthaler, M., Engelhardt, S., Schinke, B., Kobsar, A., Schmitteckert, E., Gambaryan, S., Engelhardt, C. M., Krenn, V., Eliava, M., Jarchau, T., Lohse, M. J., Walter, U. and Hein, L. (2003) Disruption of cardiac Ena-VASP protein localization in intercalated disks causes dilated cardiomyopathy. *Am. J. Physiol. Heart Circ. Physiol.* **285,** H2471-81.

Fatkin, D. and Graham, R. M. (2002) Molecular mechanisms of inherited cardiomyopathies. *Physiol. Rev.* **82,** 945-980.

Fawcett, D. W. and McNutt, N. S. (1969) The ultrastructure of the cat myocardium. I. Ventricular papillary muscle. *J. Cell Biol.* **42,** 1-45.

Feramisco, J. R., Smart, J. E., Burridge, K., Helfman, D. M. and Thomas, G. P. (1982) Co-existence of vinculin and a vinculin-like protein of higher molecular weight in smooth muscle. *J. Biol. Chem.* **257,** 11024-11031.

Ferrell, J. E.,Jr and Martin, G. S. (1989) Thrombin stimulates the activities of multiple previously unidentified protein kinases in platelets. *J. Biol. Chem.* **264,** 20723-20729.

Gallant, N. D., Michael, K. E. and Garcia, A. J. (2005) Cell adhesion strengthening: contributions of adhesive area, integrin binding, and focal adhesion assembly. *Mol. Biol. Cell* **16,** 4329-4340.

Garnier, J., Levin, J. M., Gibrat, J. F. and Biou, V. (1990) Secondary structure prediction and protein design. *Biochem. Soc. Symp.* **57,** 11-24.

Geiger, B. (1979) A 130K protein from chicken gizzard: its localization at the termini of microfilament bundles in cultured chicken cells. *Cell* **18,** 193-205.

Geiger, B., Tokuyasu, K. T., Dutton, A. H. and Singer, S. J. (1980) Vinculin, an intracellular protein localized at specialized sites where microfilament bundles terminate at cell membranes. *Proc. Natl. Acad. Sci. U. S. A.* **77,** 4127-4131.

Gilmore, A. P. and Burridge, K. (1996) Regulation of vinculin binding to talin and actin by phosphatidyl-inositol-4-5-bisphosphate. *Nature* **381,** 531-535.

Glukhova, M. A., Kabakov, A. E., Belkin, A. M., Frid, M. G., Ornatsky, O. I., Zhidkova, N. I. and Koteliansky, V. E. (1986) Meta-vinculin distribution in adult human tissues and cultured cells. *FEBS Lett.* **207,** 139-141.

Guan, K. L. and Dixon, J. E. (1991) Eukaryotic proteins expressed in Escherichia coli: an improved thrombin cleavage and purification procedure of fusion proteins with glutathione S-transferase. *Anal. Biochem.* **192,** 262-267.

Hemmings, L., Rees, D. J., Ohanian, V., Bolton, S. J., Gilmore, A. P., Patel, B., Priddle, H., Trevithick, J. E., Hynes, R. O. and Critchley, D. R. (1996) Talin contains three actin-binding sites each of which is adjacent to a vinculin-binding site. *J. Cell. Sci.* **109 (Pt 11),** 2715-2726.

Hennessey, J. P.,Jr and Johnson, W. C.,Jr. (1982) Experimental errors and their effect on analyzing circular dichroism spectra of proteins. *Anal. Biochem.* **125,** 177-188.

Huttelmaier, S., Bubeck, P., Rudiger, M. and Jockusch, B. M. (1997) Characterization of two F-actin-binding and oligomerization sites in the cell-contact protein vinculin. *Eur. J. Biochem.* **247,** 1136-1142.

Huttelmaier, S., Illenberger, S., Grosheva, I., Rudiger, M., Singer, R. H. and Jockusch, B. M. (2001) Raver1, a dual compartment protein, is a ligand for PTB/hnRNPI and microfilament attachment proteins. *J. Cell Biol.* **155,** 775-786.

Ito, S., Werth, D. K., Richert, N. D. and Pastan, I. (1983) Vinculin phosphorylation by the src kinase. Interaction of vinculin with phospholipid vesicles. *J. Biol. Chem.* **258,** 14626-14631.

Izard, T., Evans, G., Borgon, R. A., Rush, C. L., Bricogne, G. and Bois, P. R. (2004) Vinculin activation by talin through helical bundle conversion. *Nature* **427,** 171-175.

Janssen, M. E., Kim, E., Liu, H., Fujimoto, L. M., Bobkov, A., Volkmann, N. and Hanein, D. (2006) Three-dimensional structure of vinculin bound to actin filaments. *Mol. Cell* **21,** 271-281.

Johnson, R. P. and Craig, S. W. (2000) Actin activates a cryptic dimerization potential of the vinculin tail domain. *J. Biol. Chem.* **275,** 95-105.

Johnson, R. P. and Craig, S. W. (1995) The carboxy-terminal tail domain of vinculin contains a cryptic binding site for acidic phospholipids. *Biochem. Biophys. Res. Commun.* **210,** 159-164.

Johnson, R. P. and Craig, S. W. (1994) An intramolecular association between the head and tail domains of vinculin modulates talin binding. *J. Biol. Chem.* **269,** 12611-12619.

Johnson, R. P., Niggli, V., Durrer, P. and Craig, S. W. (1998) A conserved motif in the tail domain of vinculin mediates association with and insertion into acidic phospholipid bilayers. *Biochemistry* **37,** 10211-10222.

Karkkainen, S. and Peuhkurinen, K. (2007) Genetics of dilated cardiomyopathy. *Ann. Med.* **39,** 91-107.

Kioka, N., Sakata, S., Kawauchi, T., Amachi, T., Akiyama, S. K., Okazaki, K., Yaen, C., Yamada, K. M. and Aota, S. (1999) Vinexin: a novel vinculin-binding protein with multiple SH3 domains enhances actin cytoskeletal organization. *J. Cell Biol.* **144,** 59-69.

Korneeva, N. L. and Jockusch, B. M. (1996) Light microscopic analysis of ligand-induced actin filament suprastructures. *Eur. J. Cell Biol.* **71,** 351-355.

Koteliansky, V. E., Ogryzko, E. P., Zhidkova, N. I., Weller, P. A., Critchley, D. R., Vancompernolle, K., Vandekerckhove, J., Strasser, P., Way, M. and Gimona, M. (1992) An additional exon in the human vinculin gene specifically encodes meta-vinculin-specific difference peptide. Cross-species comparison reveals variable and conserved motifs in the meta-vinculin insert. *Eur. J. Biochem.* **204,** 767-772.

Krause, M., Dent, E. W., Bear, J. E., Loureiro, J. J. and Gertler, F. B. (2003) Ena/VASP proteins: regulators of the actin cytoskeleton and cell migration. *Annu. Rev. Cell Dev. Biol.* **19,** 541-564.

Kroemker, M., Rudiger, A. H., Jockusch, B. M. and Rudiger, M. (1994) Intramolecular interactions in vinculin control alpha-actinin binding to the vinculin head. *FEBS Lett.* **355,** 259-262.

Kuzmic, P. (1996) Program DYNAFIT for the analysis of enzyme kinetic data: application to HIV proteinase. *Anal. Biochem.* **237,** 260-273.

Laemmli, U. K. (1970) Cleavage of structural proteins during the assembly of the head of bacteriophage T4. *Nature* **227,** 680-685.

LaPorte, D. C., Wierman, B. M. and Storm, D. R. (1980) Calcium-induced exposure of a hydrophobic surface on calmodulin. *Biochemistry* **19,** 3814-3819.

Levin, J. M., Robson, B. and Garnier, J. (1986) An algorithm for secondary structure determination in proteins based on sequence similarity. *FEBS Lett.* **205,** 303-308.

Li, X., Romero, P., Rani, M., Dunker, A. K. and Obradovic, Z. (1999) Predicting Protein Disorder for N-, C-, and Internal Regions. *Genome Inform. Ser. Workshop Genome Inform.* **10,** 30-40.

Lifschitz-Mercer, B., Czernobilsky, B., Feldberg, E. and Geiger, B. (1997) Expression of the adherens junction protein vinculin in human basal and squamous cell tumors: relationship to invasiveness and metastatic potential. *Hum. Pathol.* **28,** 1230-1236.

Linding, R., Jensen, L. J., Diella, F., Bork, P., Gibson, T. J. and Russell, R. B. (2003) Protein disorder prediction: implications for structural proteomics. *Structure* **11,** 1453-1459.

LOWRY, O. H., ROSEBROUGH, N. J., FARR, A. L. and RANDALL, R. J. (1951) Protein measurement with the Folin phenol reagent. *J. Biol. Chem.* **193,** 265-275.

MacLean-Fletcher, S. D. and Pollard, T. D. (1980) Viscometric analysis of the gelation of Acanthamoeba extracts and purification of two gelation factors. *J. Cell Biol.* **85,** 414-428.

Maeda, M., Holder, E., Lowes, B., Valent, S. and Bies, R. D. (1997) Dilated cardiomyopathy associated with deficiency of the cytoskeletal protein metavinculin. *Circulation* **95,** 17-20.

Mandai, K., Nakanishi, H., Satoh, A., Takahashi, K., Satoh, K., Nishioka, H., Mizoguchi, A. and Takai, Y. (1999) Ponsin/SH3P12: an l-afadin- and vinculin-binding protein localized at cell-cell and cell-matrix adherens junctions. *J. Cell Biol.* **144,** 1001-1017.

Menkel, A. R., Kroemker, M., Bubeck, P., Ronsiek, M., Nikolai, G. and Jockusch, B. M. (1994) Characterization of an F-actin-binding domain in the cytoskeletal protein vinculin. *J. Cell Biol.* **126,** 1231-1240.

Miller, G. J., Dunn, S. D. and Ball, E. H. (2001) Interaction of the N- and C-terminal domains of vinculin. Characterization and mapping studies. *J. Biol. Chem.* **276,** 11729-11734.

Olson, T. M., Illenberger, S., Kishimoto, N. Y., Huttelmaier, S., Keating, M. T. and Jockusch, B. M. (2002) Metavinculin mutations alter actin interaction in dilated cardiomyopathy. *Circulation* **105,** 431-437.

Pakula, A. A. and Sauer, R. T. (1990) Reverse hydrophobic effects relieved by amino-acid substitutions at a protein surface. *Nature* **344,** 363-364.

Perez-Moreno, M., Jamora, C. and Fuchs, E. (2003) Sticky business: orchestrating cellular signals at adherens junctions. *Cell* **112,** 535-548.

Perriard, J. C., Hirschy, A. and Ehler, E. (2003) Dilated cardiomyopathy: a disease of the intercalated disc? *Trends Cardiovasc. Med.* **13,** 30-38.

Peterson, G. L. (1983) Determination of total protein. *Methods Enzymol.* **91,** 95-119.

Peterson, G. L. (1977) A simplification of the protein assay method of Lowry et al. which is more generally applicable. *Anal. Biochem.* **83,** 346-356.

Pollard, T. D. and Cooper, J. A. (1982) Methods to characterize actin filament networks. *Methods Enzymol.* **85 Pt B,** 211-233.

Richardson, P., McKenna, W., Bristow, M., Maisch, B., Mautner, B., O'Connell, J., Olsen, E., Thiene, G., Goodwin, J., Gyarfas, I., Martin, I. and Nordet, P. (1996) Report of the 1995 World Health Organization/International Society and Federation of Cardiology Task Force on the Definition and Classification of cardiomyopathies. *Circulation* **93,** 841-842.

Rodriguez Fernandez, J. L., Geiger, B., Salomon, D. and Ben-Ze'ev, A. (1993) Suppression of vinculin expression by antisense transfection confers changes in cell morphology, motility, and anchorage-dependent growth of 3T3 cells. *J. Cell Biol.* **122,** 1285-1294.

Rodriguez Fernandez, J. L., Geiger, B., Salomon, D., Sabanay, I., Zoller, M. and Ben-Ze'ev, A. (1992) Suppression of tumorigenicity in transformed cells after transfection with vinculin cDNA. *J. Cell Biol.* **119,** 427-438.

Romero, P., Obradovic, Z., Li, X., Garner, E. C., Brown, C. J. and Dunker, A. K. (2001) Sequence complexity of disordered protein. *Proteins* **42,** 38-48.

Romero, Obradovic and Dunker, K. (1997) Sequence Data Analysis for Long Disordered Regions Prediction in the Calcineurin Family. *Genome Inform. Ser. Workshop Genome Inform.* **8,** 110-124.

Rudiger, M., Korneeva, N., Schwienbacher, C., Weiss, E. E. and Jockusch, B. M. (1998) Differential actin organization by vinculin isoforms: implications for cell type-specific microfilament anchorage. *FEBS Lett.* **431,** 49-54.

Saga, S., Hamaguchi, M., Hoshino, M. and Kojima, K. (1985) Expression of meta-vinculin associated with differentiation of chicken embryonal muscle cells. *Exp. Cell Res.* **156,** 45-56.

Sambrook, J., Fritsch, E. F. and Maniatis, T. (1989) *Molecular cloning: A laboratory manual,* Cold Spring Harbor Laboratory Press, New York.

Saucier, A. C., Mariotti, S., Anderson, S. A. and Purich, D. L. (1985) Ciliary dynein conformational changes as evidenced by the extrinsic fluorescent probe 8-anilino-1-naphthalenesulfonate. *Biochemistry* **24,** 7581-7585.

Saunders, R. M., Holt, M. R., Jennings, L., Sutton, D. H., Barsukov, I. L., Bobkov, A., Liddington, R. C., Adamson, E. A., Dunn, G. A. and Critchley, D. R. (2006) Role of vinculin in regulating focal adhesion turnover. *Eur. J. Cell Biol.* **85,** 487-500.

Schwehm, J. M., Kristyanne, E. S., Biggers, C. C. and Stites, W. E. (1998) Stability effects of increasing the hydrophobicity of solvent-exposed side chains in staphylococcal nuclease. *Biochemistry* **37,** 6939-6948.

Shackelford, D. A. and Zivin, J. A. (1993) Renaturation of calcium/calmodulin-dependent protein kinase activity after electrophoretic transfer from sodium dodecyl sulfate-polyacrylamide gels to membranes. *Anal. Biochem.* **211,** 131-138.

Siliciano, J. D. and Craig, S. W. (1987) Properties of smooth muscle meta-vinculin. *J. Cell Biol.* **104,** 473-482.

Steimle, P. A., Hoffert, J. D., Adey, N. B. and Craig, S. W. (1999) Polyphosphoinositides inhibit the interaction of vinculin with actin filaments. *J. Biol. Chem.* **274,** 18414-18420.

Steiner, R. F. (1984) Location of a binding site for 1-anilinonaphthalene-8-sulfonate on calmodulin. *Arch. Biochem. Biophys.* **228,** 105-112.

Strasser, P., Gimona, M., Herzog, M., Geiger, B. and Small, J. V. (1993) Variable and constant regions in the C-terminus of vinculin and metavinculin. Cloning and expression of fragments in E. coli. *FEBS Lett.* **317,** 189-194.

Stryer, L. (1965) The interaction of a naphthalene dye with apomyoglobin and apohemoglobin. A fluorescent probe of non-polar binding sites. *J. Mol. Biol.* **13,** 482-495.

Subauste, M. C., Pertz, O., Adamson, E. D., Turner, C. E., Junger, S. and Hahn, K. M. (2004) Vinculin modulation of paxillin-FAK interactions regulates ERK to control survival and motility. *J. Cell Biol.* **165,** 371-381.

Sun, N., Critchley, D. R., Paulin, D., Li, Z. and Robson, R. M. (2008) Human alpha-synemin interacts directly with vinculin and metavinculin. *Biochem. J.* **409,** 657-667.

Towbin, H., Staehelin, T. and Gordon, J. (1979) Electrophoretic transfer of proteins from polyacrylamide gels to nitrocellulose sheets: procedure and some applications. *Proc. Natl. Acad. Sci. U. S. A.* **76,** 4350-4354.

Turner, C. E. and Burridge, K. (1989) Detection of metavinculin in human platelets using a modified talin overlay assay. *Eur. J. Cell Biol.* **49,** 202-206.

Vasile, V. C., Will, M. L., Ommen, S. R., Edwards, W. D., Olson, T. M. and Ackerman, M. J. (2006) Identification of a metavinculin missense mutation, R975W, associated with both hypertrophic and dilated cardiomyopathy. *Mol. Genet. Metab.* **87,** 169-174.

Volberg, T., Geiger, B., Kam, Z., Pankov, R., Simcha, I., Sabanay, H., Coll, J. L., Adamson, E. and Ben-Ze'ev, A. (1995) Focal adhesion formation by F9 embryonal carcinoma cells after vinculin gene disruption. *J. Cell. Sci.* **108 (Pt 6),** 2253-2260.

Weekes, J., Barry, S. T. and Critchley, D. R. (1996) Acidic phospholipids inhibit the intramolecular association between the N- and C-terminal regions of vinculin, exposing actin-binding and protein kinase C phosphorylation sites. *Biochem. J.* **314 (Pt 3),** 827-832.

Weiss, E. E., Kroemker, M., Rudiger, A. H., Jockusch, B. M. and Rudiger, M. (1998) Vinculin is part of the cadherin-catenin junctional complex: complex formation between alpha-catenin and vinculin. *J. Cell Biol.* **141,** 755-764.

Weller, P. A., Ogryzko, E. P., Corben, E. B., Zhidkova, N. I., Patel, B., Price, G. J., Spurr, N. K., Koteliansky, V. E. and Critchley, D. R. (1990) Complete sequence of human vinculin and assignment of the gene to chromosome 10. *Proc. Natl. Acad. Sci. U. S. A.* **87,** 5667-5671.

Witt, S., Zieseniss, A., Fock, U., Jockusch, B. M. and Illenberger, S. (2004) Comparative biochemical analysis suggests that vinculin and metavinculin cooperate in muscular adhesion sites. *J. Biol. Chem.* **279,** 31533-31543.

Wood, C. K., Turner, C. E., Jackson, P. and Critchley, D. R. (1994) Characterisation of the paxillin-binding site and the C-terminal focal adhesion targeting sequence in vinculin. *J. Cell. Sci.* **107 (Pt 2),** 709-717.

Xu, W., Baribault, H. and Adamson, E. D. (1998) Vinculin knockout results in heart and brain defects during embryonic development. *Development* **125,** 327-337.

Yu, J. W., Mendrola, J. M., Audhya, A., Singh, S., Keleti, D., DeWald, D. B., Murray, D., Emr, S. D. and Lemmon, M. A. (2004) Genome-wide analysis of membrane targeting by S. cerevisiae pleckstrin homology domains. *Mol. Cell* **13,** 677-688.

Zamir, E. and Geiger, B. (2001) Molecular complexity and dynamics of cell-matrix adhesions. *J. Cell. Sci.* **114,** 3583-3590.

Zemljic-Harpf, A. E., Ponrartana, S., Avalos, R. T., Jordan, M. C., Roos, K. P., Dalton, N. D., Phan, V. Q., Adamson, E. D. and Ross, R. S. (2004) Heterozygous inactivation of the vinculin gene predisposes to stress-induced cardiomyopathy. *Am. J. Pathol.* **165,** 1033-1044.

Ziegler, W. H., Liddington, R. C. and Critchley, D. R. (2006) The structure and regulation of vinculin. *Trends Cell Biol.* **16,** 453-460.

Ziegler, W. H., Tigges, U., Zieseniss, A. and Jockusch, B. M. (2002) A lipid-regulated docking site on vinculin for protein kinase C. *J. Biol. Chem.* **277,** 7396-7404.

Zieseniss, A., Schroeder, U., Buchmeier, S., Schoenenberger, C. A., van den Heuvel, J., Jockusch, B. M. and Illenberger, S. (2007) Raver1 is an integral component of muscle contractile elements. *Cell Tissue Res.* **327,** 583-594.